

NATIONAL RADIO ASTRONOMY OBSERVATORY
GREEN BANK, WEST VIRGINIA

ELECTRONICS DIVISION INTERNAL REPORT No. 184

REFLECTION MEASUREMENTS ON THE
140-FOOT AND 300-FOOT RADIOTELESCOPES

J. RICHARD FISHER

JANUARY 1978

NUMBER OF COPIES: 150

NATIONAL RADIO ASTRONOMY OBSERVATORY

REFLECTION MEASUREMENTS ON THE
140-FOOT AND 300-FOOT RADIOTELESCOPES

J. Richard Fisher

Summary

A 3.3 GHz swept frequency reflectometer has been used at the prime focus of the 140-foot and 300-foot telescopes to identify sources of reflection which cause frequency dependent antenna gain and noise spectra on the scale of a few MHz. This fine scale structure in the frequency domain of the antenna response is in many cases the limiting factor in detection and measurement of microwave spectral lines from cosmic radio sources.

Measurements on the 140-foot show that the primary sources of reflection are the roof and miscellaneous metal on top of the Cassegrain radiometer house, the Cassegrain feeds, the inner portion of the main reflector, and the circumferential gaps between the panels in the main reflector. The 300-foot measurements show a strong reflection from the center of the dish with at least three multiple bounces between the main reflector and the focal cabin. Studies have been made of several metallic spoiler surfaces, and some success has been had in reducing the reflections on the 140-foot and in identifying sources of multiple reflections on the 300-foot.

Wideband noise spectra have been measured with various NRAO radiometers on the 140-foot, and qualitative agreement between these spectra and the reflectometer results has been obtained.

The mechanics of the reflectometer technique are gone into in some detail, but later sections can be read without going into this detail.

Introduction

The problem of "baseline ripple" or "baseline curvature" has plagued radio astronomical measurements since the first spectral line was discovered in 1952, but because the causes have been many and complex they have not been well understood. By "baseline" we mean the intensity of radiometer output as a function of frequency in the absence of narrowband cosmic radiation. Generally the problem has been circumvented by subtracting reference spectra taken under similar conditions at a spot in the sky not containing a radio emitter, "fitting" the baseline with a polynomial, or moving the radiometer feed focal position to phase-cancel dish reflections. These methods tend to waste observing time or lead to spurious results. Until a few years ago the roots of the problem had been only randomly attacked.

Baseline problem causes are many: e.g., radiometer passband drift, telescope RF cable mismatches, local oscillator leakage, frequency dependent receiver temperature, and reflections or standing waves in the telescope structure. The latter manifests itself in several ways by distorting the frequency structure of ground radiation, the receiver noise itself, solar radiation in the antenna sidelobes and continuum radiation from a source in the main beam. Studying these various effects with standard radiometric spectrometers can be very frustrating because of the long integration times involved and the difficulty of disentangling the different effects. An interesting compendium of baseline anomalies was recently written by Lockman and Rickard [1].

No one has yet succeeded in reasonably complete cancellation of prime focus telescope reflections at more than a few isolated frequencies although a fair number of internal observatory reports have been written on the subject. Morris [2], [3] has written two mathematical treatments of telescope reflections. Reports and memos dealing mainly with observations of spectrometer

baselines and some trials of spoilers in the center of paraboloids are by Weinreb [4], [5]; Padman [6], [7]; and Beiging and Pankonin [8]. Some other reports which apparently pertain to the subject and have been referred to by the above authors are written by Morris [9]; Poulton [10], [12]; Padman [11]; and Gardner [13]; but I have not seen any of these reports. Experimental radiometric work has been done at the secondary focus of two-reflector telescopes by Wilson and Hills [14] and Ulich [15] with the latter having success at canceling secondary mirror reflections near 100 GHz with a controlled reflector plate.

In an attempt to unravel various telescope reflections Morris and Beiging [16], [17] and we have been making swept frequency reflectometer measurements from the prime focus of our respective telescopes. This report outlines the work at the NRAO and makes a few comparisons with the 100-meter results at the M.P.I.f.R.

The Measurement Technique

The purpose of swept frequency reflectometry is to separate reflections occurring at different distances from the signal source. This is done by transmitting a CW signal and measuring the amplitude and phase with respect to the source of the returned wave over a reasonably wide band of frequencies.

The Fourier transform of this amplitude and phase versus frequency is then a function of return amplitude versus distance from the source. The basic principle is that the farther a reflection is from the source the faster the phase of its returned wave will change with frequency. Descriptions of this technique as applied to waveguide measurements are given by Holloway [18] and Somlo [19] among others, and its application dates back at least to 1925 in ionospheric measurements (cf. Appleton and Barnett [20]). As far as I know

the first application to radio astronomy antennas was at the M.P.I.f.R. in Bonn [16], [17].

The test setup used in this study is shown in Figure 1. Instead of directly measuring the phase of the returned wave it is added to a sample of the outgoing wave, and the voltage vector sum is measured. After subtraction of a DC term this is equivalent to measuring the cosine component of the complex return wave voltage. For this purpose the sine component is redundant.

The data acquisition and reduction is controlled by an HP 9825A desktop calculator. It feeds a BCD encoded frequency to the NRAO universal local oscillator (ULO) consisting of an HP 5105A 0-500 MHz synthesizer and a X4 frequency multiplier. This in turn sends an L-band signal to the prime focus box where it is amplified, frequency doubled, and amplified to be fed into a dual directional coupler type reflectometer and then to a wideband corrugated horn (return loss and beamshapes shown in Figure 2). The outgoing wave directional coupler pickup is sent to a level detector to keep the transmitted amplitude constant and to a hybrid for addition to the return voltage. The linear sum is rectified by a square law detector and sent down the telescope on a shielded pair cable to an integrating type digital voltmeter. The calculator reads and stores the DVM output (typically 1 second integration) and then sets a new frequency.

To start a measurement run the total bandwidth, number of sample points, starting frequency and high pass data filter distance are keyed into the calculator. It then collects the amplitude vs. frequency data and stores them in internal memory. The square roots of the DVM readings are taken to convert them to amplitudes, and then they are passed through a digital high pass filter to attenuate the large return from the feed. To eliminate end effects of the filter process, data are taken beyond either end of the desired bandwidth.

The digital high pass actually consists of a truncated error function-sinc product low pass represented by

$$\frac{\sin \pi x}{\pi x} \exp [(-\pi (x/2)^2)] \Big|_{x=-2}^{+2}$$

convolved with the data, and the result is subtracted from the original data. Figure 3 shows the cutoff characteristics of this filter. The filtered data are plotted on the X-Y plotter for inspection, and the calculator then proceeds with the transform.

Before performing the Fourier transform the data are weighted with a half cycle of a sine function with zeros at either end of the frequency range to reduce the transform sidelobes. The transform algorithm is adapted from a FORTRAN version by Brenner [21].

A Fourier transform of N real unsymmetric data points produces $N/2 + 1$ power spectrum points with minimum sampling in the frequency and distance or delay domains. Hence, 256 data points give 129 return power versus distance points. However, with minimum sampling density the power spectra are a bit difficult to interpret by eye because depending on the exact distance of the reflection the return power can either appear all in one data point or be distributed between two adjacent points each being smaller in amplitude than the single point. This makes the reflection amplitude appear to bob up and down with small distance changes so I elected to over sample in the distance coordinate by factor of two. This is wasteful of computer storage space because a number of zeros equal to the number of data points must be added to the data field making the transform twice as large, but there was still room in the calculator for a 257 point (129 minimum sampling) output spectrum which was sufficient for most purposes. With 256 non-zero data points the transform took

about 50 seconds. Toward the end of the reported measurements the calculator memory was doubled so 512 point output spectra were available on the last 300-foot run.

Figure 4 shows the 256-point "instrumental profile" with sine function data weighting for a reflection unresolved in distance. In the actual measurements the sidelobes tend to be lower because most reflections are partially resolved. It will also be seen that in the presence of several very strong reflections the large-distance background noise can get quite strong (as much as -20 dB relative to the main signals). This may be due to slight nonlinearities in the detector system causing intermodulation of the various signals.

Note in Figure 4 as in all succeeding spectra that the vertical scale is logarithmic with a nonlinearity on the bottom end. Since a log scale is unbounded a small arbitrary quantity was added to all power values. Above about -80 dB the scale is essentially constant. Keep in mind also that in a discrete transform it is generally assumed that no reflections exist beyond the largest displayed distance. If they do they will alias back into the spectrum and cause confusion. This can be a problem with multiple reflections on the telescope.

Calibrations

Return loss intensity calibrations rely on the nominal values of attenuators and coupling coefficients of the components in Figure 1. The overall calibration accuracy should be about ± 2 dB, and it was felt that more accuracy than this was not necessary. Back of the envelope calculations of the expected return from a 1 meter diameter flat test reflector agreed with the measured value to within a few dB.

Because the phase reference in the reflectometer is not at the phase center of the feed the computed distances are not the distances from the feed. The distance offset was measured to be 0.5 ± 0.1 meters with a flat calibration reflector at a known distance. This offset must be subtracted from the distances shown on the figures to follow to get the true feed-reflector distance.

Spoiler Tests

In addition to calibration tests a considerable number of reflection trials with the system were made on the ground before putting the device on the telescope both to get a feel for the vagaries of the system and to try several methods of spoiling reflections. The test configuration is shown in Figure 5.

Three basic spoiler configurations were tried: a flat disk, a cone, and a steep-sided multipyramid surface (Figure 6). As shown in Figure 5 each was mounted on a rotatable platform and return loss was measured as a function of angle with respect to the feed-reflector line. The tilt and rotation of the flat disk were adjusted for maximum reflected power and its return loss was used as a reference. The results are shown in Figures 7, 8, and 9.

It is clear that the smallest return is obtained from the tilted disk. This seems reasonable since this reflector has a smooth phase variation of currents on its surface, and no edges are along constant phase lines. I suspect that a tilted square at the same angle would cause a higher reflection than the disk if two of its edges were nearly perpendicular to the feed-reflector line.

Three cone opening angles were tried as seen in Figure 8. The angle was changed by overlapping adjacent sectors of a sheet metal disk, so as the height

of the cone increased the projected diameter decreased, but this should not affect the general conclusions to be drawn from Figure 8. The steeper cones have a smaller return when face-on, but rise to a maximum when one side becomes perpendicular to the line of sight. Return loss at very large rotation angles are similar to those for the disk. The main disadvantage of the face-on cone is that the outer edge is a discontinuity along a constant phase line.

The pyramidal surface is the poorest spoiler of the three. The configuration tried was a rather periodic surface, so the surface current phases were not well randomized. The return from a perfectly isotropic scatterer of one meter cross section would be about 30 dB below the face-on disk.

Some generalizations about good spoilers might be as follows: (1) Smooth surfaces are better than irregular ones as long as none of the surface is nearly perpendicular to the line of sight. (2) Discontinuities in the surface (edges, bends, cracks) should not follow lines of constant phase for long distances. (3) Long, slender reflectors should have their long dimension tilted away from the source. I suspect that if the long dimension is perpendicular to the line of sight and the short dimension is smaller than a wavelength (e.g., a pipe) changing the short dimension cross sectional shape will not substantially change the reflection intensity. It might be better to cover a narrow object with a large flat reflector with no edges perpendicular to the line of sight.

During the tests with the flat, 1-meter disk the reflection properties of the equipment box itself (a standard NRAO prime focus box) were tested by looking for a double bounce return (feed-reflector-box-reflector-feed path). At a reflector distance of 10 meters from the face-on disk the double bounce was 25 dB below the first return which had a 47 dB return loss. The double bounces were easily eliminated by covering the sections of the box which were parallel to the reflector with absorber. Reflections from the feed itself were not strong enough to be measurable.

140-Foot Telescope Measurements

Two sessions were available for reflection tests on the 140-foot telescope: May 1977 and September 1977.

A schematic of the 140-foot telescope cross section is shown in Figure 10. A detailed view of the top of the Cassegrain house is shown in the Figure 11 photograph. The L-band feed is temporarily covered with a tilted aluminum square in this picture. The feed support legs are cylindrical members 38 cm in diameter, and the bottom of the feed support ring is a tubular ring about 3 meters across inside of which are mounted various surfaces and motors for attachment and movement of front end boxes.

For all of the 140-foot tests a ring of absorber covered the front of the reflector electronic box and its mounting ring to minimize possible confusion due to double bounce reflections. Most reflection scans were from 3.05 to 3.70 GHz with 256 samples giving a distance range of about 29 meters one way. The distance from the focal point to the edge of the dish is less than 25 meters. A high pass cutoff of 5 meters was used in all cases.

A first look at the 140-foot gave the return loss-distance spectrum shown in Figure 12. As mentioned earlier the presence of relatively strong returns around 13 meters apparently enhanced the noise level at large distances. Four strong returns are immediately apparent and can be identified from their distances. Reflection A comes from the air ducts, feed mounts and other miscel- lany above the Cass house roof, and B comes from the roof itself. Spike C is the result of waves entering the long Cassegrain feeds and being reflected from the L-band termination (poor match at 3 GHz) or the waveguide cutoff di- mension at 3 GHz in the C, Ku, and K band feeds. Return D is from the inner surface of the dish around the Cass house. All of these reflection sources fit the measured distance to better than 30 cm or so.

The causes of reflections A, B, and C were further confirmed by covering the appropriate areas with absorber. The result of putting the flat spoiler seen in Figure 11 over the L-band feed and absorber over the rest of the objects on the Cass roof is shown in Figure 13. The dashed line outlines the reflection intensities before adding absorber and the spoiler. We also tried removing covers from the feeds one at a time to measure their relative contributions. Reflection C had a return loss of 58 dB with the L-band feed uncovered, 65 dB with the C-band uncovered, and 78 dB with just the Ku-band feed uncovered as compared to 54 dB with all feeds exposed.

A more permanent fix for the reflections from the top of the Cass house was to install a tilted aluminum reflector during the September 1977 measurements above the roof with removable covers for Cassegrain work. The schematic side view of this cover is shown in Figure 14, and the resulting reflection spectrum is shown in Figure 15. The cover was bent in the center to reduce its height at the south end. The highest remaining peak around 15 meters is probably due to a bit of as yet uncovered metal on the east side of the house.

With the attenuation of reflections A, B, and C in Figure 13 a couple of other features pop out of the noise. Peaks E and F fit the distances of the roughly 8 mm wide inner and outer circumferential gaps between the surface panels. Covering the outer gap with sticky aluminum foil reduced reflection F by about 8 dB, but covering the inner gap was inconclusive. The rather insignificant gaps might seem unlikely candidates for strong reflectors, but they are discontinuities at the same phase for quite a long distance. A possible reason that reflection F did not completely disappear when the outer gap was covered is that the level of the intermediate and outer panels do not match well so that although the current gap is bridged by the foil there is still a small phase discontinuity at the gap.

The reflection zone around D and E is a muddled one. The phase error pattern on the inner portion of the dish produced by diffraction around the Cass house roof is probably a complicated one, and the situation is not helped by the inner gap. The individual peaks in this distance region are not easily interpreted. Figure 16 shows the effect of changing the axial position of the transmitting feed by 55 cm. In one case there are two peaks at approximately -64 dB and in the other there are three peaks around -68 dB. I do not believe this effect can be due to interaction of the sidelobes of two reflections, but it is difficult to rule out. Many of the reflection peaks seen on the 100-meter telescope by Morris and Bieging were interpreted as involving reflections from the feed support structure onto the dish surface and back to the feed. Such effects could be involved in the reflection complex around peaks D and E although the 140-foot feed supports are not nearly as massive as those on the 100-meter dish.

In any event reducing the reflections from the inner surface of the dish over a wide range of frequencies is not easy. Even if the full set of inner panels and the Cass house were removed the reflection at the distance of the inner gap would be as strong as the present inner panel reflection because of the discontinuity at the inner edge of the intermediate panels. The reason a reflection is not seen from the outer edge of the dish is that the illumination is down by about 17 dB which reduces the reflection by 34 dB and puts it in the noise. One could imagine putting a jagged spoiler in the center of the dish so that the edge of the "hole" is not along a constant phase line, but to do a proper job of tapering the hole at 21 cm the spoiler would cover a large portion of the center of the aperture.

One solution to the inner surface reflections is to tune them out at the frequency being used at any given time. This requires a controllable reflector

near the center of the dish to create a return equal in amplitude and out of phase with the dish reflection. A reasonably good cancellation can probably be realized over a 50 MHz bandwidth. This bandwidth is limited by the fact that the inner surface reflections are spread over about one meter in distance. The amplitude of the compensating reflection could be controlled either by changing the size of the reflector, or having two reflectors which partially cancel one another by putting them partially out of phase. The latter would be mechanically easier to implement.

Some experimenting with manually adjusted reflectors was done in September 1977. The main result was to find that, even for two people, adjusting these plates from the surface of the dish is extremely tedious. Some sort of remote control from the control room will have to be devised. We also looked at the phase of the reflected wave pattern from the dish itself as a function of telescope position. To within an accuracy of about 20° at 3 GHz the phase did not vary as the telescope was moved from zenith to horizon. This indicates that reflector adjustments would not need to be made often during an observing run at one frequency.

With the reduction of some of the stronger reflections a few more weak returns become apparent in Figure 15. Reflection G is from the stiffening cables near their attachment point at the mid-point of the feed support legs. This was verified by changing the axial position of the feed by 90 cm and seeing that the distance change of peak G was only about 70 cm which is consistent with the cosine of the angle of the feed support legs (34°). It is a bit curious that this reflection was not seen earlier such as in Figure 13, but this may be a good example of how careful one must be in interpreting signals near the noise threshold.

Reflection I in Figure 15 is from the edge of the dish. It is at the proper distance and moves about half the amount of the feed axial position change which is consistent with its being 60° off the telescope axis. I have not determined the source of peaks H, J, or K. They all move at the same speed as the feed in the axial direction indicating that they are near the axis of the dish, but they are much further away than the surface. They are not aliased into the spectrum from larger distances because then they would move in the opposite direction from the focus change, unless they are further away than 60 meters which seems unlikely. If they were the result of harmonics generated in the measuring instrument they should move twice as fast as the focus change. I cannot think of a likely combination of double reflections which could produce any of the three peaks.

Radiometer Noise Spectra on the 140-Foot

To be reasonably certain that the reflections measured with the 3 GHz reflectometer are the main source of baseline ripples a few radiometer noise spectra measurements were made at 1.4, 1.6, 3.3, 8.5, and 10.6 GHz. The results are shown in Figures 17 through 23.

Composite spectra with bandwidths from 80 to 130 MHz were constructed by stepping the 10 MHz autocorrelator bandpass along in 8 MHz steps, and the individual spectra were matched at the common end frequencies. Most of the spectra are "total power" differences between two measurements taken with the antenna pointed at the zenith and the feed at focal positions $\lambda/8$ above and below the nominal focal point. The resulting spectra are mainly the interference of ground radiation entering the feed directly and via scattering from the feed support ring onto the dish surfaces and back to the feed. This is not the normal cause of baseline ripples since most observing procedures

tend to cancel its effect, but it was the only external source of noise strong enough to see with short integration times necessary to cover a wide spectrum.

Measurements of a continuum source were made at 1.6 and 8.5 GHz by differencing "total power" on-source and off-source spectra at the same focal positions. These are shown in Figures 20 and 22 and will be discussed later.

The bottom halves of Figures 17 and 18 show the $\pm \lambda/8$ focus difference spectra for the two orthogonal linear polarization channels of the L-band section of the 6/25 cm receiver. At the top of these plots are the Fourier transforms of the spectra. The transforms show the main features seen with the reflectometer: the top of the Cass house and the dish surface, and possibly the Cassegrain feeds, the outer gap, and the dish edge. Figure 21 is a similar set of plots for 3.3 GHz where the top of the Cass house, the Cassegrain feeds and the dish surface are clearly visible.

Figures 19, 22a, and 23 show difference spectra for $\pm \lambda/8$ focal positions at 1.6, 8.5, and 10.5 GHz. Either not enough data were available or there was too large a low frequency component in these spectra to make a useful transform, but the same general features are seen at these frequencies as were seen at 1.4 and 3.3 GHz. The amplitude of the ripples in these spectra depend on the spillover of the feeds, but no attempt has been made to interpret this bit of information.

Figures 20 and 22b are composites of on-off spectra of a continuum source at 1.6 and 8.5 GHz. At least at 1.6 GHz in Figure 20 there is a ripple component with peak-to-peak spacings which are characteristic of the telescope reflections. However, there is a much stronger large scale curvature component in these spectra. This curvature is probably due to the addition of wide band noise from the radio source which, when the on and off spectra are normalized by the autocorrelator, causes the relative noise contributions from different

parts of the front end passband to be different and not cancel in the subtraction. Also, variation of the feed transfer characteristics with frequency could distort the continuum spectra slightly and cause the observed curvature. Unfortunately, I did not record the antenna temperature of the 3C 147.1 at 8.5 GHz so ripple amplitude comparisons are not very useful.

300-Foot Telescope Reflectometry

The focal ratio of the 300-foot telescope is the same as the 140-foot, but there the similarity ends. The focal length of the 300-foot is 38.7 meters compared to 18.3 meters on the 140-foot. There is no Cassegrain house on the 300-foot, and there are many more tiers of surface panels than on the 140-foot. As seen in Figures 24 and 25 the feed support structure is two north-south bridgework legs which are 1.37 meters across on the inside of the legs, and the base of the feed cabin is 2.1 x 2.7 meters between the feed legs. Part of the feed cabin and a walkway extend into the leg structure in a plane perpendicular to the telescope axis.

Two sets of 300-foot telescope measurements were made in July and December 1977. The December measurements were made with additional memory in the calculator which permitted better distance resolution so all reflection spectra shown are from the December run.

Figure 26 shows the reflection spectrum of the 300-foot before any modifications were made to reduce reflections. The number of data points is 512 instead of 256 so the relative resolution is a factor of two better than that shown in Figure 4. In Figure 26 three harmonics plus the main reflection are visible. As will be shown later the harmonics are due to multiple bounces between the dish vertex and the underside of the feed cabin. The high noise level between 40 and 70 meters is again possibly due to slight nonlinearities in the detection circuitry.

Figure 27 is an expanded look at the main vertex reflection with the harmonics folded back but not overlapping the fundamental. The bottom half of this figure is with the feed nearest the vertex, and the top is with the feed's focal position 87 cm further from the vertex. Peak A fits the distance to the vertex very well, but the origins of features B and C are not yet determined. These could be produced by reflections from the feed support legs to the surface and back to the feed or by circumferential gaps between the inner surface panels. Feature C nearly disappeared with the feed farthest from the dish vertex, but B did not change its position relative to the main return. The circumferential panel gaps on the 300-foot are composed of straight line segments as opposed to being perfect circles as on the 140-foot which may explain why this source of reflection is not as prominent as it was on the 140-foot.

So far most of the experimentation with absorbers and spoilers on the 300-foot has been aimed at reducing the multiple reflections. Three ways of reducing these reflections were tried: absorber under the feed cabin, tilted reflectors at the vertex and metal screen under the top part of the feed support legs. As on the 140-foot a ring of absorber covered the dish side of the reflectometer equipment box during all measurements.

Figure 28 shows the result of placing a 2.5 (N-S) x 3.4 (E-W) meter absorber panel under the feed cabin with a 1.4 meter square hole in the center to let the equipment box stick through. This panel was large enough to cover all of the feed cabin between the feed support leg attachment points. Some of the harmonic components were substantially reduced. (The broken lines show the reflections without absorber.) Enough tests on the measurement system had been performed to be reasonably confident that the harmonics were not due to detector nonlinearities, but the results in Figure 28 show conclusively

that the harmonics are a property of the telescope since the main reflection did not change.

Another method of reducing the multiple reflections was tried, but only a low resolution spectrum of the result is available (Figure 29). In this experiment a 3.7 (N-S) x 3.0 (E-W) meter area of metal screen tilted 18° to the west from the horizontal was placed at the center of the dish. Reduction of the multiple reflections was about as good as if not slightly better than that realized with absorber under the feed cabin.

Both the absorber panels under the feed cabin and the tilted screen at the vertex left a relatively strong first harmonic and a weak second harmonic reflection component. In both trials the walkways north and south of the feed cabin and the traveling feed rails were left uncovered. An attempt was made to shield the walkways with metal screen hung under the top of the feed support legs from the north and south edges of the absorber panels to a distance of about 6 meters down each leg. Unfortunately this screen tended to flop around in the breeze which caused a time variable reflectometer return. This raised the reflection spectrum noise level as can be seen in Figure 30. However, the first harmonic is still visible at about the same level as with the absorber alone. Apparently the walkways are not the strongest remaining contributors to the second bounce features.

While the absorber panel and the screens under the walkways were in place the tilted metal screen at the vertex was divided into three 1.2 x 3.0 meter sections and placed on the surface directly under the traveling feed track. The traveling feed track extends 7 meters on either side of the center of the feed cabin. Each section was again tilted 18° from the horizontal toward the west. The three sections covered about 50% of the projected area of the traveling feed track but the effect on the remaining first harmonic component

was negligible as shown in Figure 31. More screen to cover the full traveling feed track projection will have to be tried before anything conclusive can be said about this potential source of reflection, however.

Before any of the absorber or screens were put on the telescope a set of reflection measurements were made with the feed at different east-west positions on the Sterling mount track. (The Sterling mount is separate from the traveling feed track and is used to track sources with receivers above 1 GHz up to 2^{m} either side of the meridian. The reflectometer box was installed in the Sterling mount.) The results are shown in Figure 32. The top spectrum is taken with the feed 38 cm west of center and the bottom with the feed 38 cm east of center. In this figure the arrow marks the position of the first harmonic peak in Figure 31. This peak shows a strong dependence on the east-west position of the feed which indicates that the source of this reflection is rather extended in the east-west direction. The traveling feed track fits this description.

The strong hour angle dependence of the multiple reflections can be seen when watching a radiometer spectrum of a source without continuum radiation build up in the "total power" mode with the autocorrelator. First a 4-minute reference spectrum is taken on an adjacent point in the sky by tracking over the full Sterling mount range. As the on-source position is tracked the spectral baseline looks very ragged in the beginning when the first 20^{s} integration is subtracted from the full 4-minute reference spectrum. As the source is tracked the baseline ripples change rather dramatically until the last 40 or 20 seconds' worth of data is added when the baseline suddenly flattens out.

Conclusions

The 140-foot telescope is a complicated structure in terms of reflections. Six sources of reflection have been identified: metal atop the Cassegrain house, the Cassegrain feeds, the dish surface, circumferential gaps in the surface, the edge of the dish, and stiffening cables on the feed support legs. The first three are by far the most important, and the first two have been reduced by more than 20 dB with a metal spoiler on the top of the Cass house. Reflections from the gaps were reduced by covering them with aluminum tape, but a more permanent solution must be found since the tape peels up with thermal contraction of the surface panels.

On the 300-foot telescope the direct reflection from the center of the dish is the most prominent feature in its reflection spectrum. Two weaker reflections involving slightly larger path lengths are seen but have not been identified, yet. The feed cabin plays a strong role in creating multiple reflections between it and the vertex. Even though these higher order reflections are weaker than the main one they are quite important in spectral line observations because they cause fine scale structure in the baselines. We had some success in reducing the multiple reflections with spoiler screens at the vertex or absorber under the feed cabin, but somewhat larger spoiler areas must be tried to completely identify and suppress the multiple reflections.

Attenuation of the first reflection from the inner dish surface of either telescope will require a rather large spoiler in the center of the dish or tuning plates to selectively compensate for the telescope reflections at the observing frequency. The spoiler may have to be so large that a significant portion of the dish collecting area will be lost, particularly on the 140-foot. The tuning plate approach suffers from its relative complexity and the need for adjustment every time the observing frequency is changed. The main

surface reflection on both telescopes seems to be reasonably independent of telescope position so an elaborate computer controlled servo for the tuning plates would not be needed, but some sort of convenient adjustment from the control room would be necessary.

So far all of the identified reflection paths involve a single reflection source with the exception of the multiple bounce harmonics on the 300-foot. This is quite different from the interpretation of most of the reflection peaks on the 100-meter telescope by Morris and Bieging [16], [17]. We do see structure in the distance range just beyond that of the center of the main dish which could involve reflections from the feed support structure, but more work remains to be done to see if such is the case.

Observations of instrumental noise spectra indicate that the reflectometer tests are aimed in the right direction. Naturally one cannot cover a wide range of frequencies with the sensitivity normally attained in spectral line work to show a direct improvement in baselines with each telescope modification. Observations of a couple of strong continuum sources show baseline structure characteristic of the measured reflection distances, but other baseline effects are present at the same time. Their solution is also important.

Acknowledgements:

With some thought I can trace most of the ideas contained in this report to bits of conversations with many people or to partially forgotten pieces of literature read over the last few years. Just a few examples are: conversations with John Armstrong and Russ Hulse on fast Fourier transforms; a Hewlett-Packard note on swept frequency reflectometry; John Brooks' remarks about reflections from steps in the surface of the 210-foot at CSIRO, and a Bill Brundage speculation about reflections from the Cassegrain feeds. Dave Morris

of the MPI sent me a thoughtful letter on many aspects of his work which were not included in the referenced reports after talking to John Findlay about some of my work.

John Ralston and Omar Bowyer designed the sheet metal work and the Green Bank shop put it together. The telescope operators and Herb Hanes' crew made the many telescope modifications. Bill Kuhlken constructed the reflectometer and helped with the measurements. Carolyn Dunkle, Tony Miano and the Green Bank photographics group put this report together.

References:

- [1] Lockman, F.J. and Rickard, L. J, "Spurious Spectral Features at the NRAO 140-Foot Telescope", NRAO Electronics Division Internal Report No. 183, December 1977.
- [2] Morris, D., "Chromatism at Millimeter Wavelengths", Rapport technique provisoire, G.I. mm/DM/No. 125, 10 April 1973.
- [3] Morris, D., "Chromatism in Radio Telescopes due to Blocking and Feed Scattering", internal report, Observatoire de Paris, 92190 Meudon, France, date unknown.
- [4] Weinreb, S., "Effect of Feed-Paraboloid Reflections upon Line Receiver Performance on the 140-ft Telescope", NRAO memo, 14 November 1967.
- [5] Weinreb, S., "Effect of 140' Vertex Cone on Spectral-Line Baselines", NRAO memo, 22 May 1970.
- [6] Padman, R., "Report on Baseline Ripple - 64 m Dish", CSIRO internal report, 22 January 1976.
- [7] Padman, R., "Reduction of Baseline Ripple on Spectra Recorded with the Parkes 64 m Radio Telescope", CSIRO preprint RPP 2094, 1977.
- [8] Bieging, J. and Pankonin, J., "Experimental Investigations of the Causes of Spectroscopic Baseline Ripple at 5 GHz", M.P.I.f.R. Technischer Bericht No. 16.
- [9] Morris, D., "Chromatism and Antenna Design", Internal Report G.I. mm No. 125a, 1974.
- [10] Poulton, G.T., "Minimization of Spectrometer Ripple in Prime Focus Radiotelescopes", CSIRO Research Report, 1974.
- [11] Padman, R., CSIRO Division of Radiophysics Report RPP 2056(L), 1977.
- [12] Poulton, G.T., "An Investigation into Ripple Causing Mechanisms in a Large Two Reflector Telescope", Queen Mary College, London, 1975.

- [13] Gardner, F.F., "An Investigation of Instrumental Effects with Spectral Line Observations with the 100 m Telescope", M.P.I.f.R. Internal Report, 1973.
- [14] Wilson, T.L. and Hills, R.E., "The Instrumental Frequency Baseline of the 100-meter Telescope from the Secondary Focus at 11 cm", M.P.I.f.R. Technischer Bericht No. 11.
- [15] Ulich, B.L., "Telescope Standing Waves: Their Causes and Cures", National Radio Science Meeting, Boulder, Colorado, January 1978.
- [16] Morris, D. and Beiging, J., "Progress Report on Baseline Ripple Problem", M.P.I.f.R. internal report, 20 January 1976.
- [17] Bieging, J. and Morris, D., "Further Efforts to Improve the Spectroscopic Baseline of the 100-meter Telescope", M.P.I.f.R. internal report, 6 December 1976.
- [18] Holloway, D.L., "The Comparison Reflectometer", IEEE Trans. MTT-15, No. 4, 250, April 1967.
- [19] Somlo, P.I., "The Locating Reflectometer", IEEE Trans. MTT-20, No. 2, 105, February 1972.
- [20] Appleton, E.V. and Barnett, M.A.F., "Local Reflection of Wireless Waves from the Upper Atmosphere", Nature, Vol. CXV, 333, March 7, 1925.
- [21] Brenner, N., "The Fast Fourier Transform", Astrophysics Part C, Radio Observations, Ed. M. L. Meeks, Academic Press, New York, 1976.

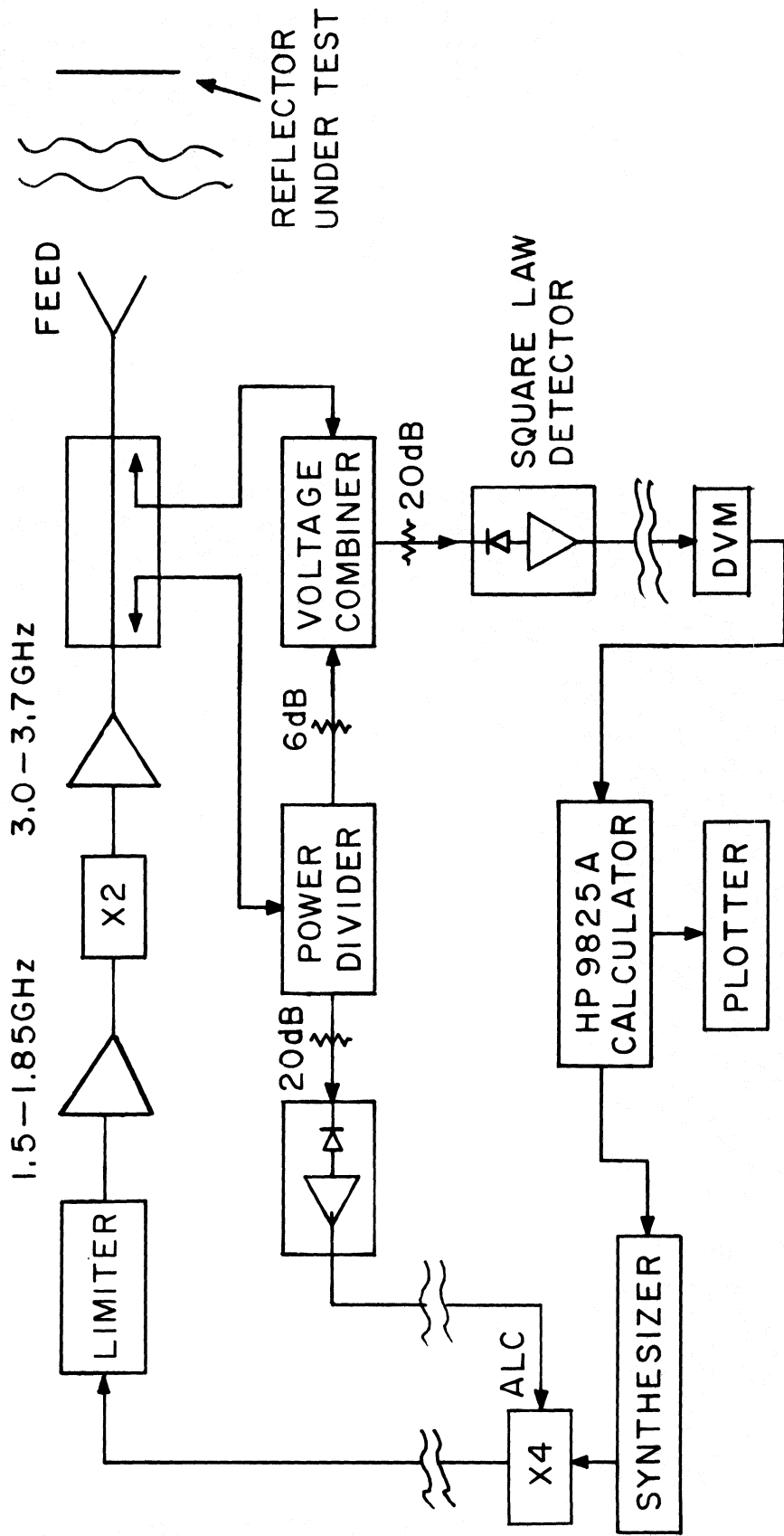


FIGURE 1. SWEEPED FREQUENCY REFLECTOMETER TEST SETUP.

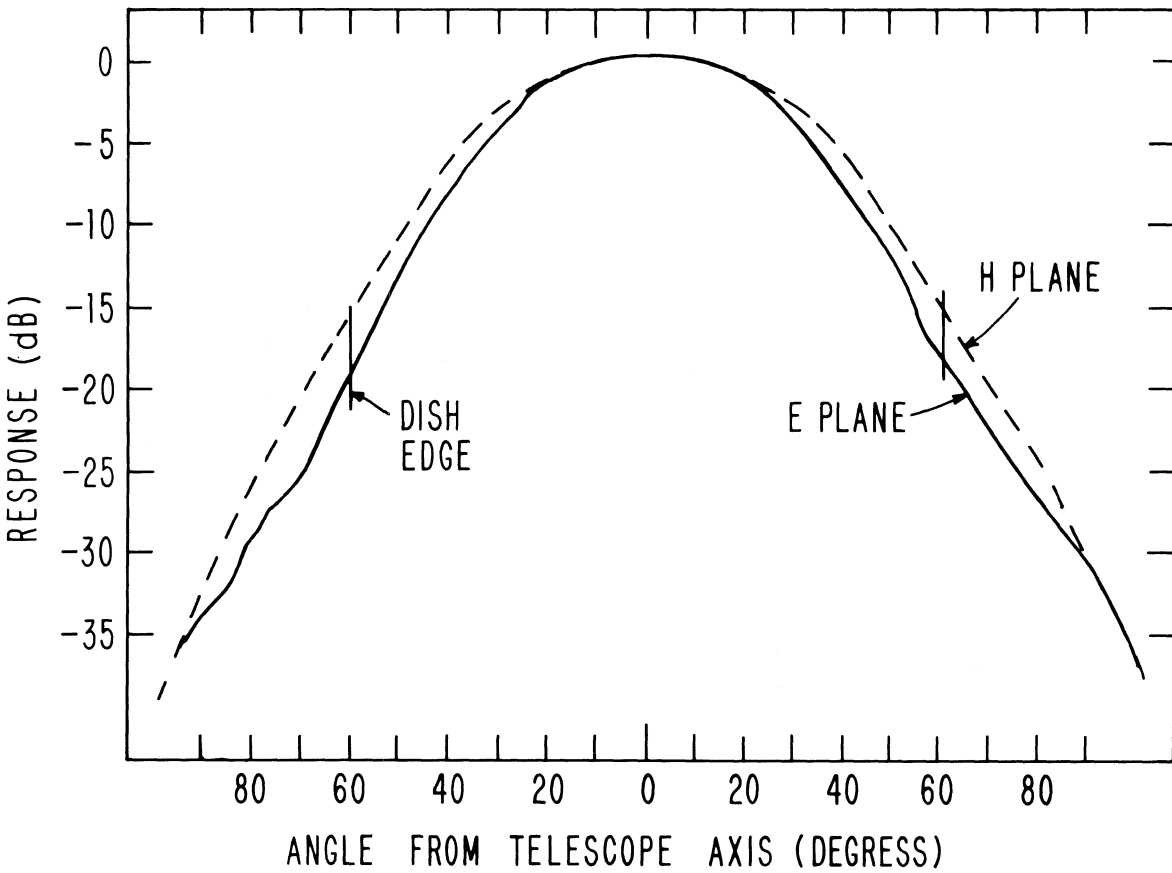
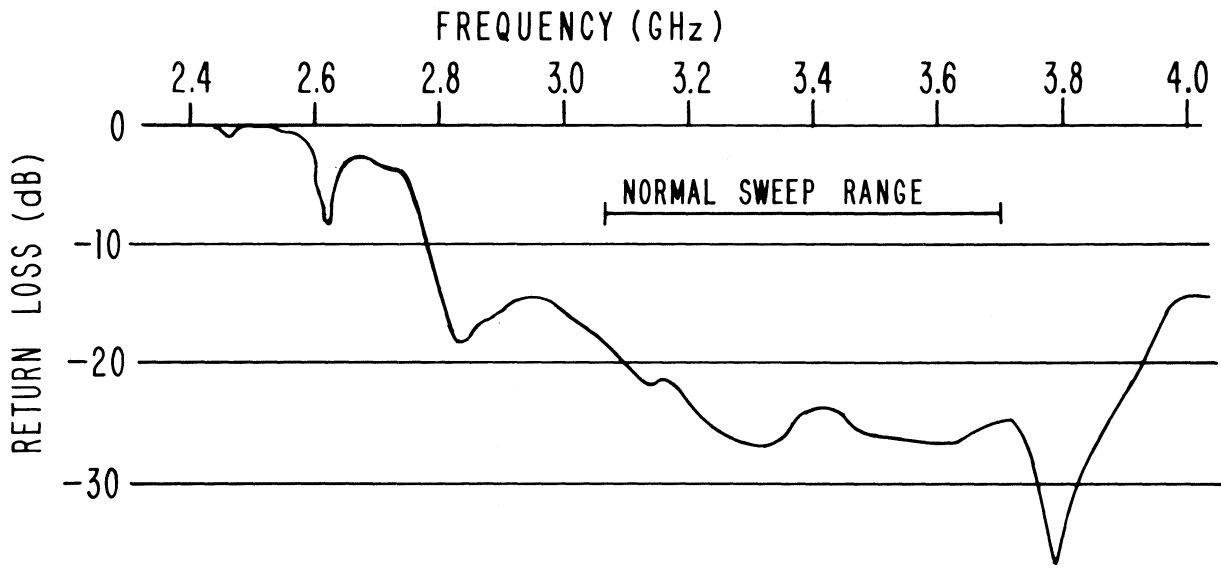


FIGURE 2. CHARACTERISTICS OF THE FEED USED FOR REFLECTION MEASUREMENTS. THE TOP FIGURE IS THE REFLECTION AMPLITUDE FROM THE FEED AND THE BOTTOM IS THE FEED PATTERN.

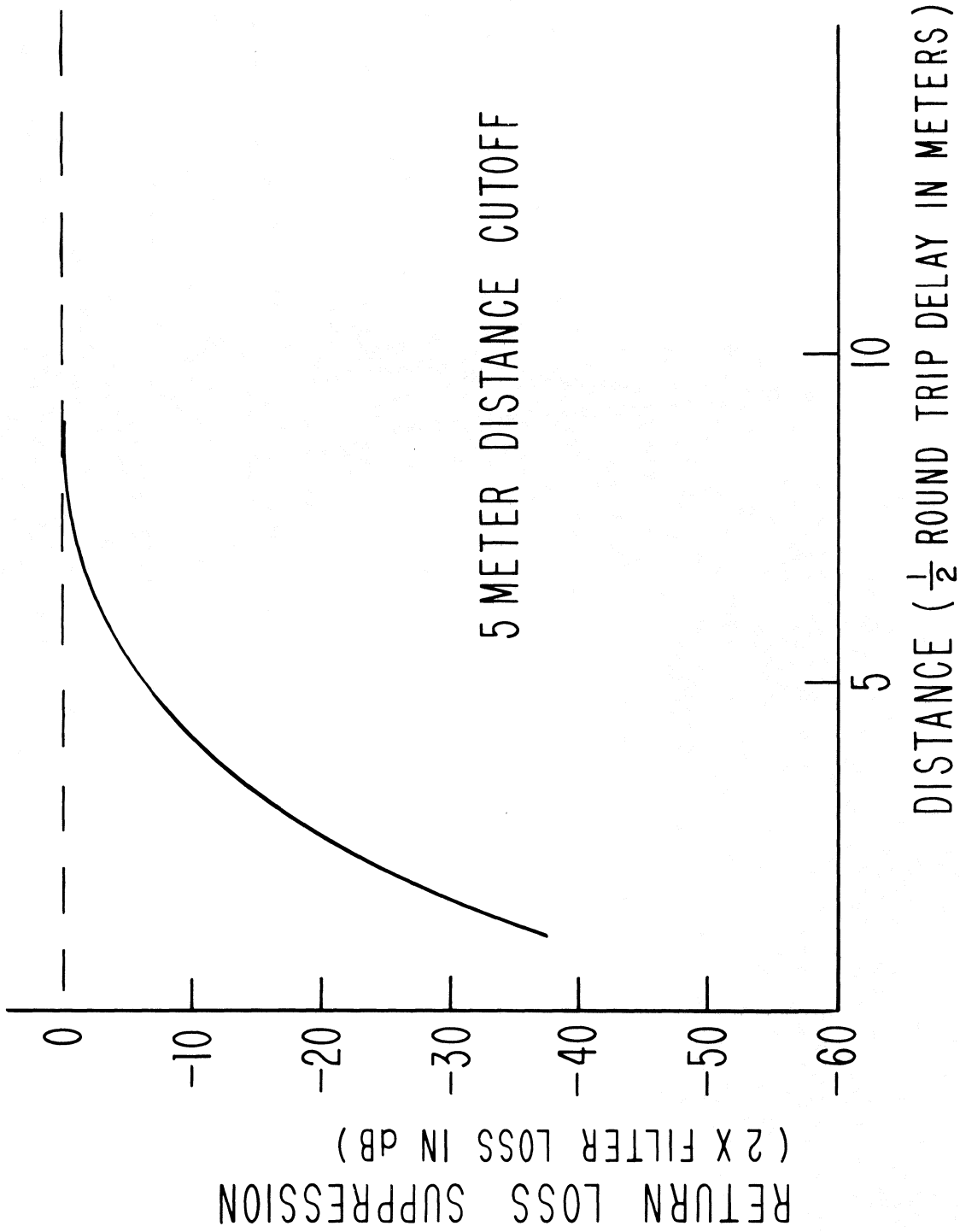


FIGURE 3. RESPONSE OF THE DIGITAL HIGH PASS FILTER USED TO SUPPRESS THE LARGE FEED REFLECTION.

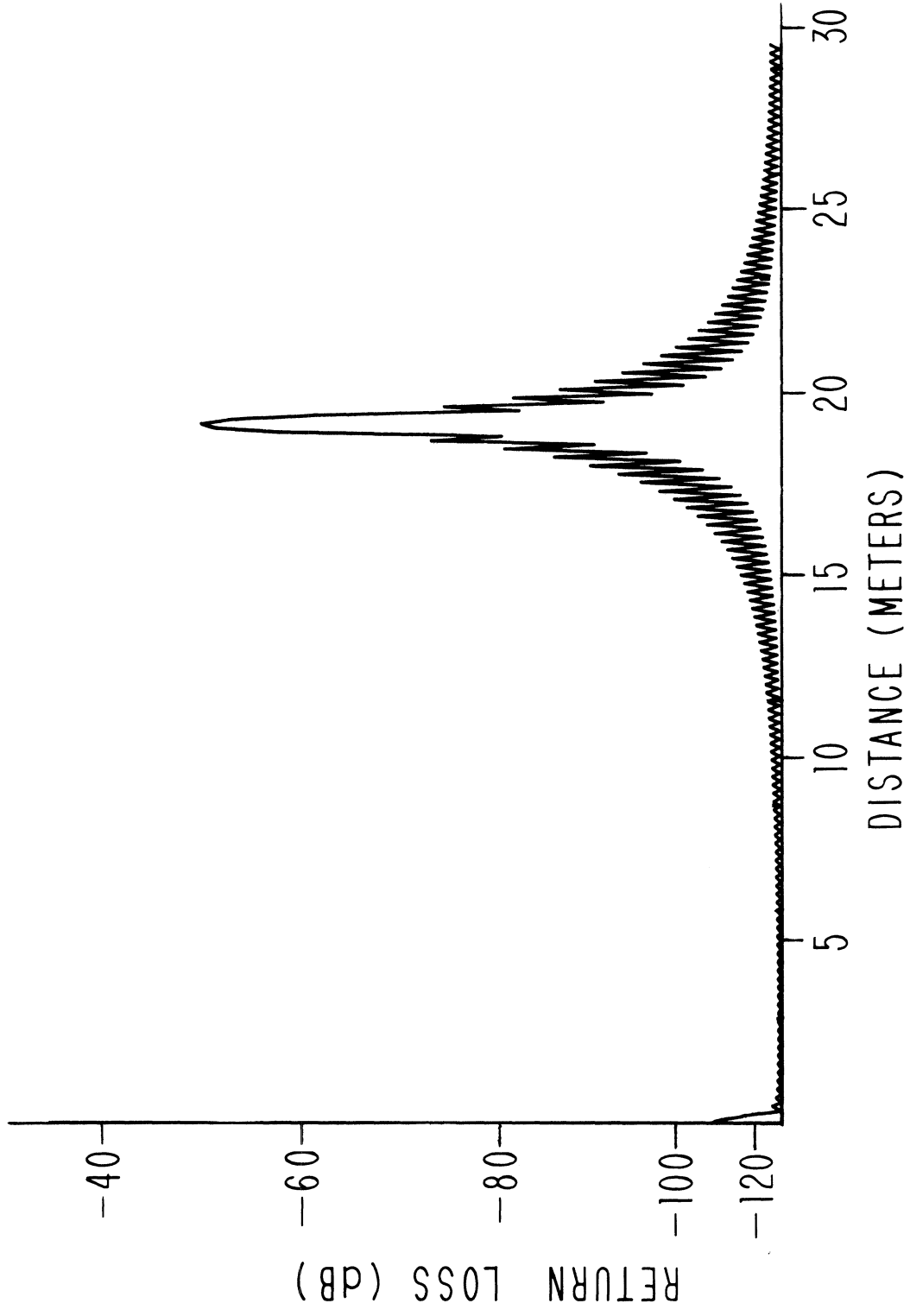


FIGURE 4. INSTRUMENTAL RESPONSE TO A SINGLE UNRESOLVED REFLECTION WITH 256 AMPLITUDE-FREQUENCY SAMPLES.

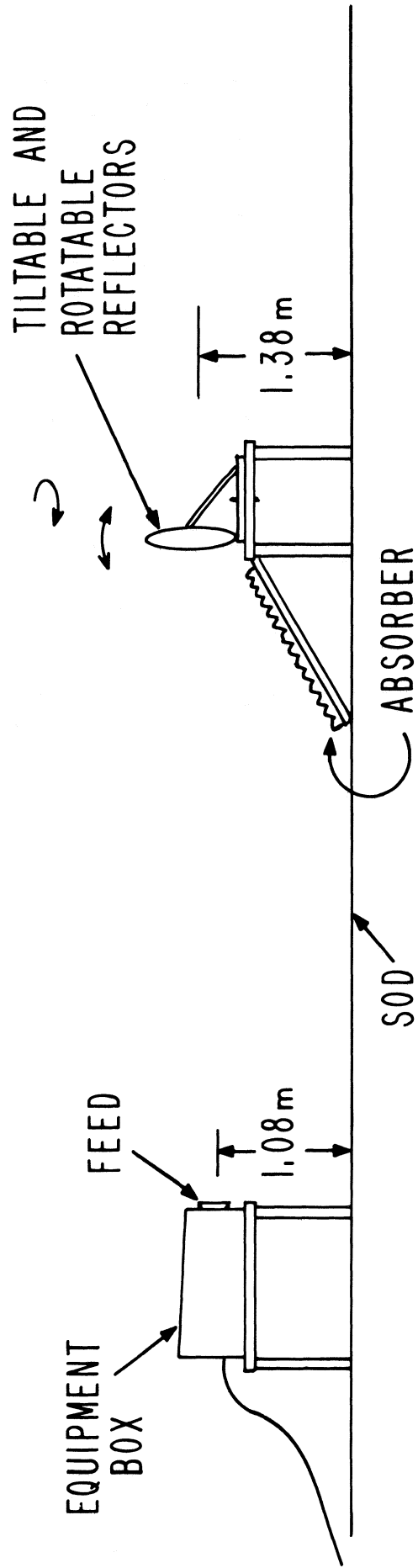
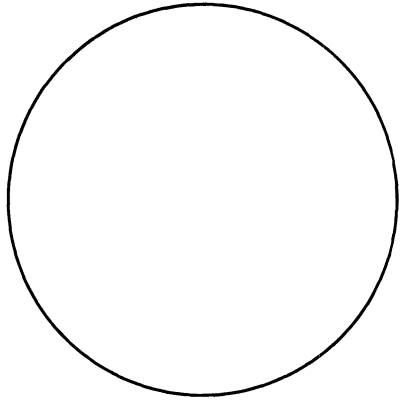
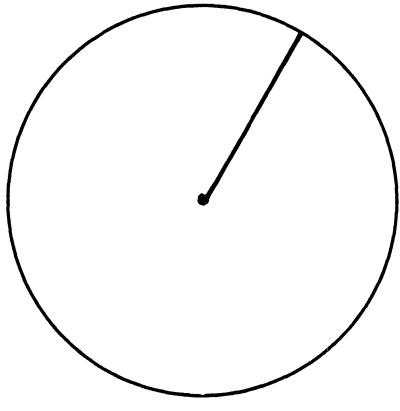
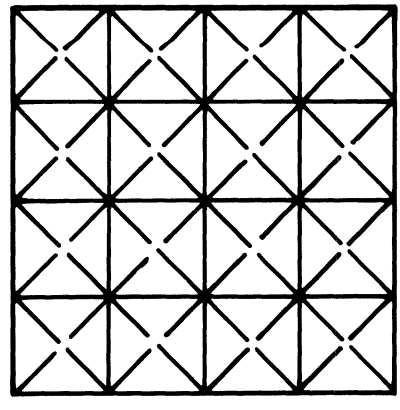


FIGURE 5. CALIBRATION AND SPOILER TEST SETUP.

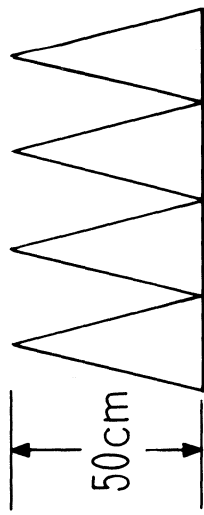


FRONT

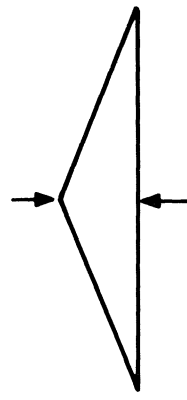
1 METER

~ 1 METER

1 METER



50cm



VARIABLE
HEIGHT

SIDE



DISK

CONE

PYRAMID SURFACE

FIGURE 6. THREE SPOILER CONFIGURATIONS TRIED IN TEST SETUP SHOWN IN FIGURE 5.

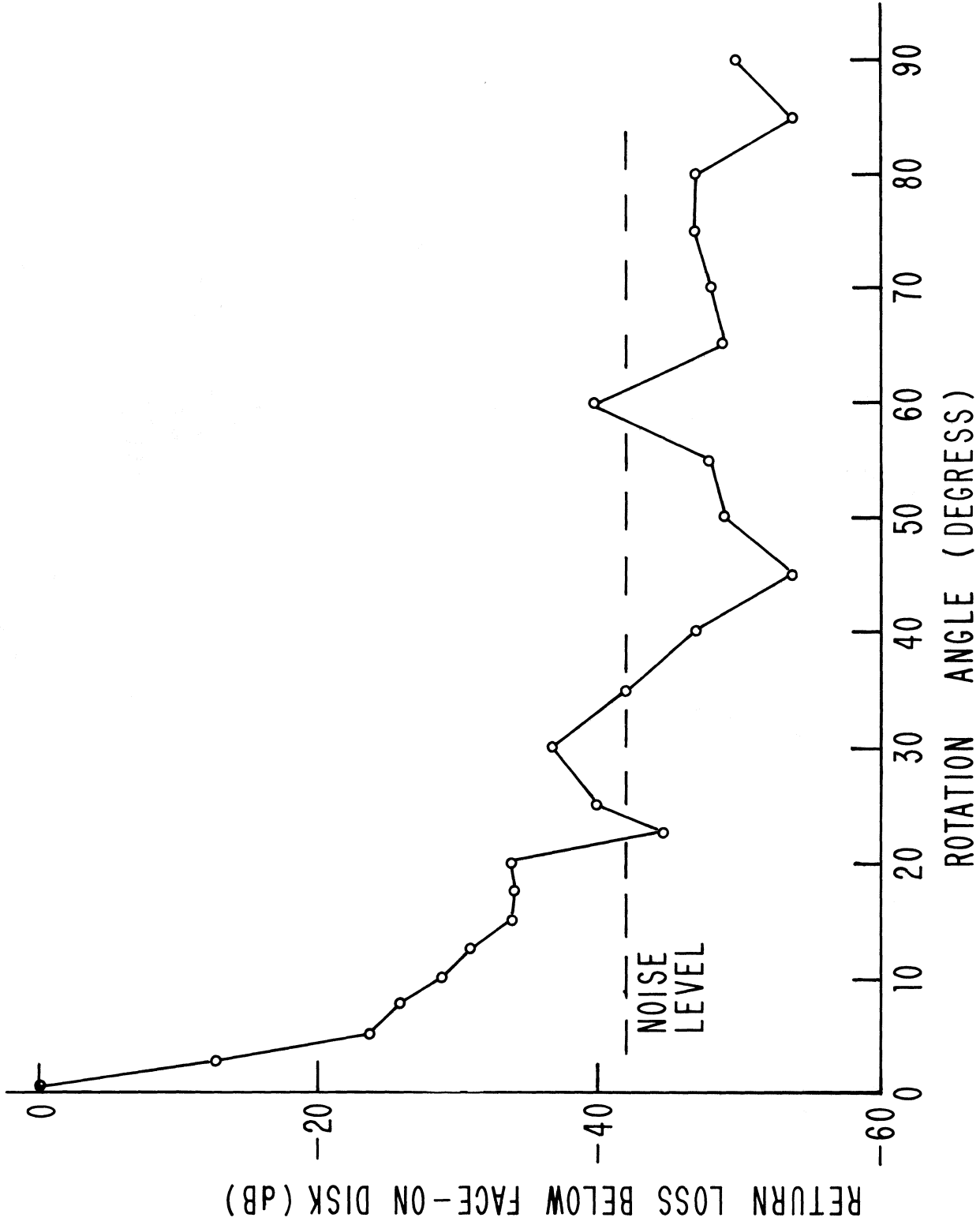


FIGURE 7. RELATIVE REFLECTION AMPLITUDE FROM THE 1-METER DIAMETER DISK AS A FUNCTION OF TILT TO THE LINE OF SIGHT. (ZERO DEGREES IS FACE-ON.)

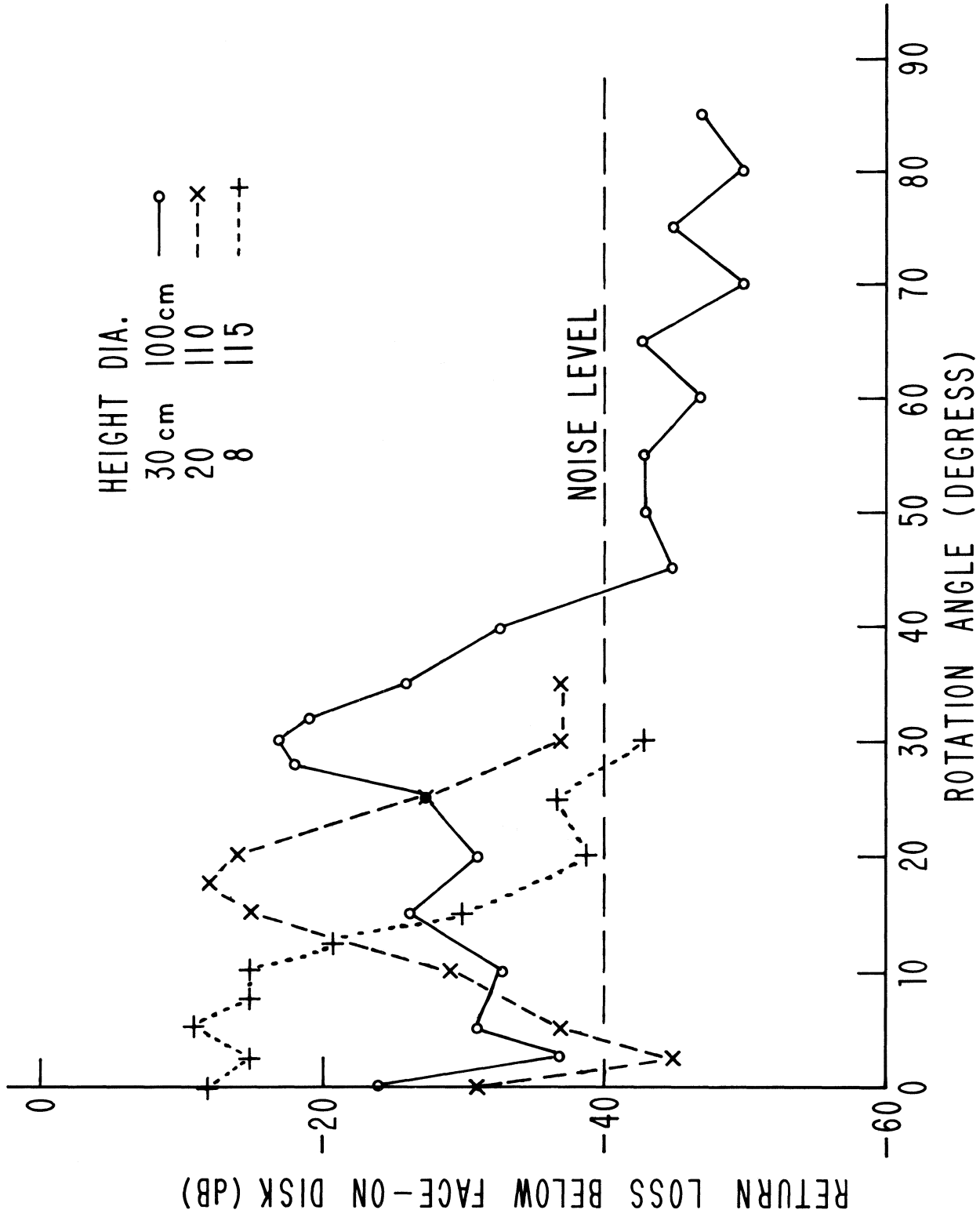


FIGURE 8. REFLECTION AMPLITUDE RELATIVE TO FACE-ON DISK FROM THREE CONES OF DIFFERENT OPENING ANGLES AS A FUNCTION OF TILT TO THE LINE OF SIGHT. THE HEIGHT AND DIAMETER OF EACH ARE GIVEN AT THE TOP RIGHT.

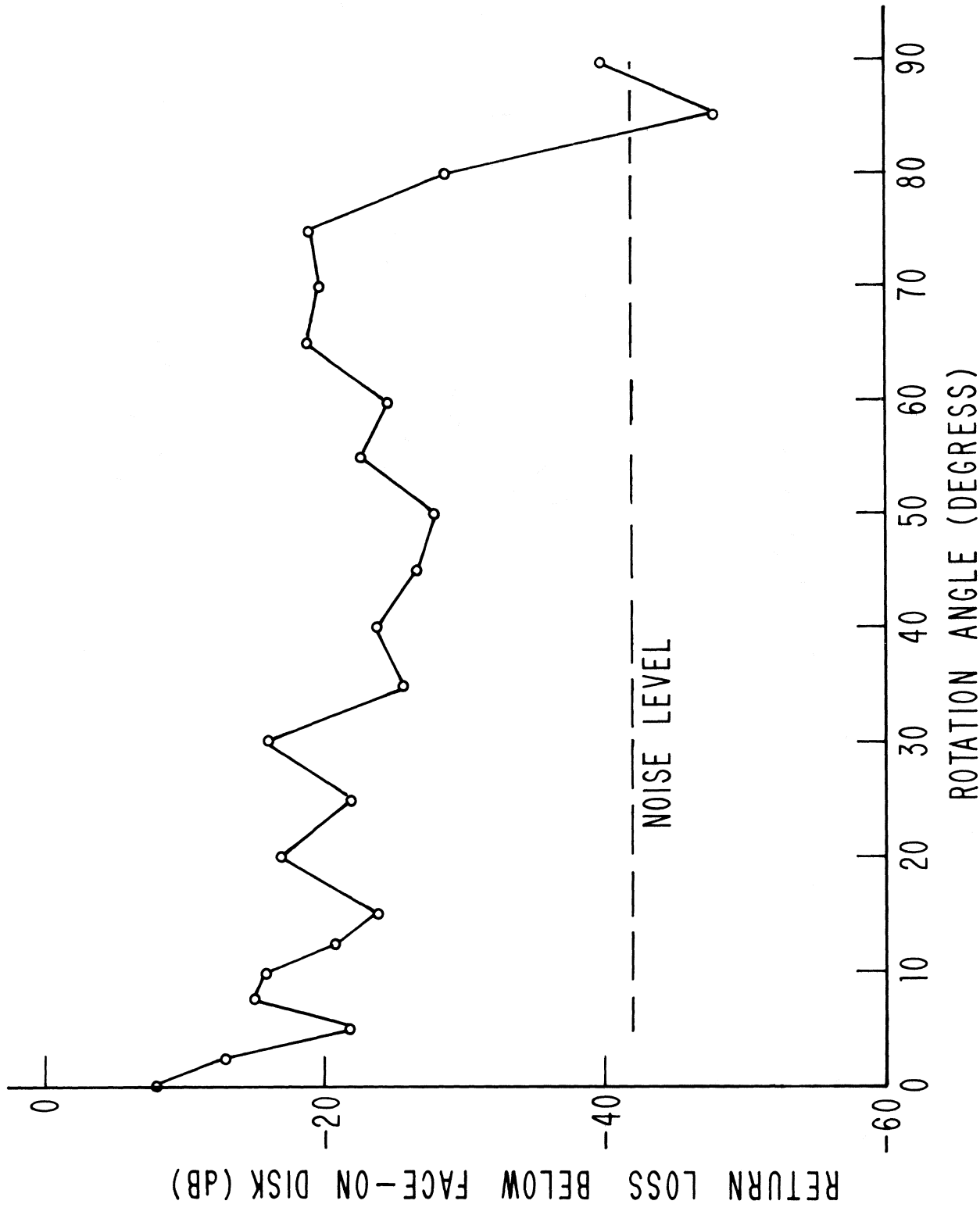


FIGURE 9. REFLECTION AMPLITUDE RELATIVE TO FACE-ON DISK FROM THE PYRAMIDAL SURFACE SHOWN IN FIGURE 6 AS A FUNCTION OF TILT TO THE LINE OF SIGHT.

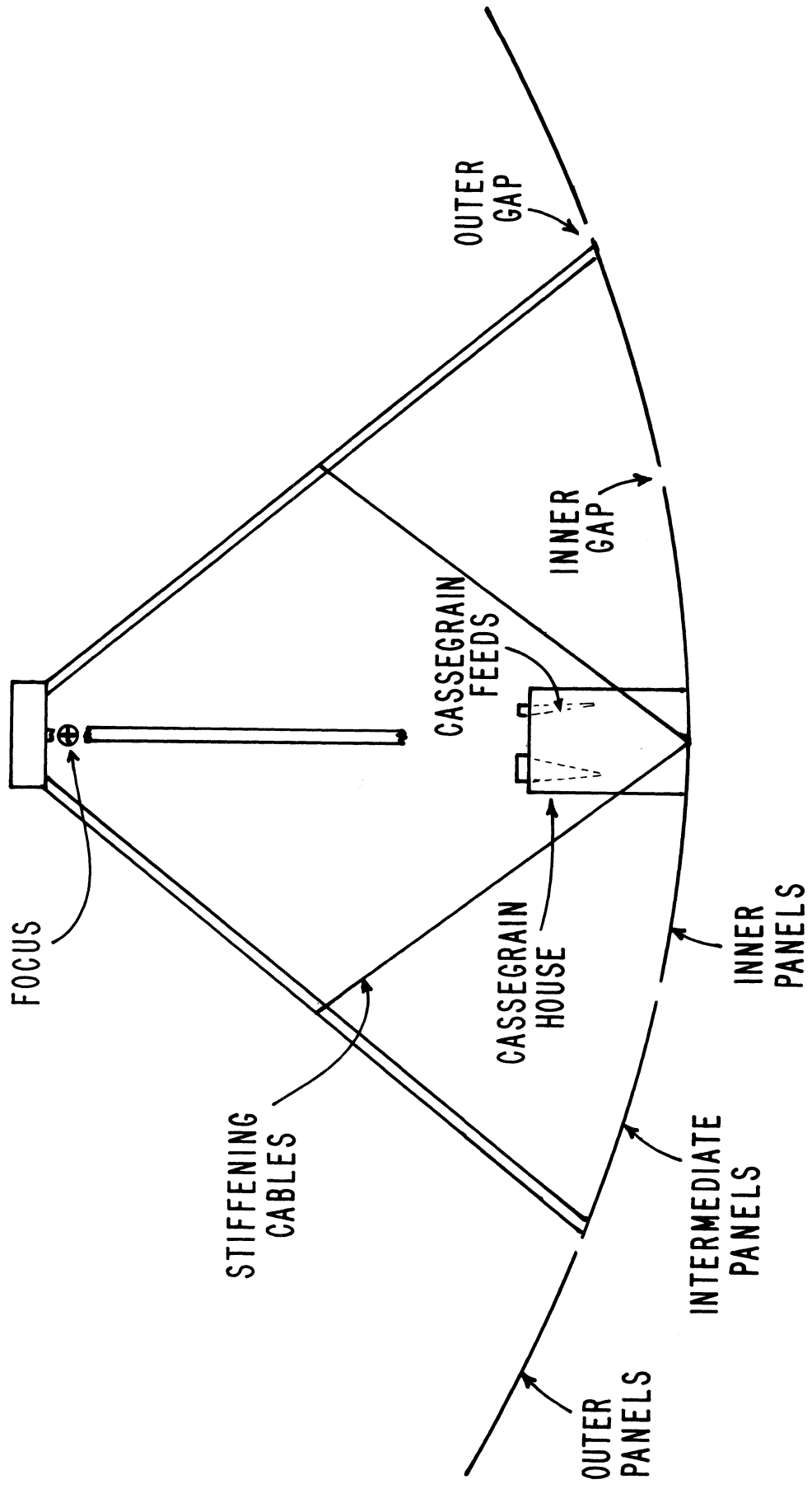


FIGURE 10. SCHEMATIC CROSS SECTION OF THE 140-FOOT TELESCOPE. THERE ARE FOUR FEED SUPPORT LEGS WITH STIFFENING CABLES RUNNING FROM THE CENTER OF EACH TO THE BASE OF ADJACENT LEGS.

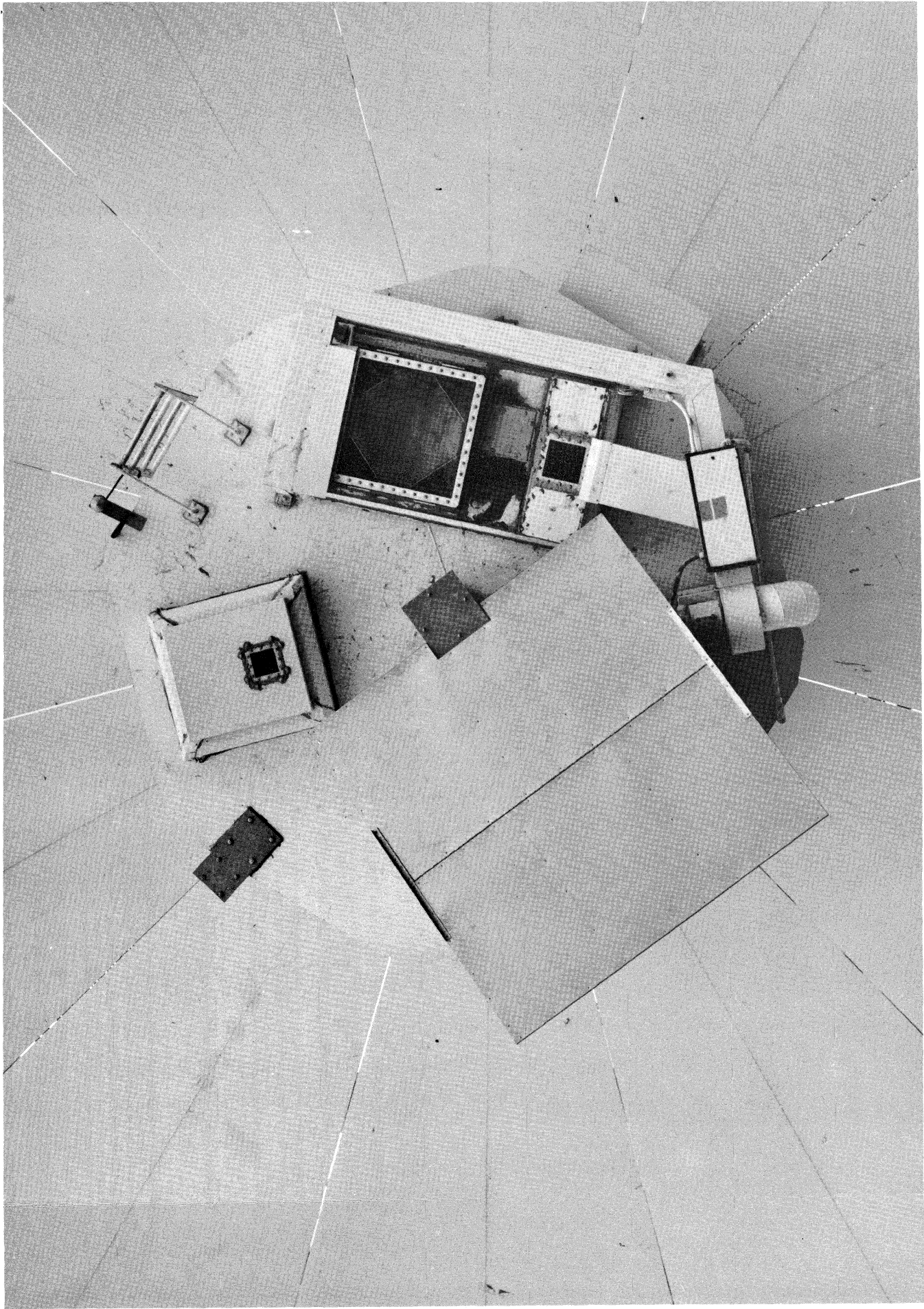
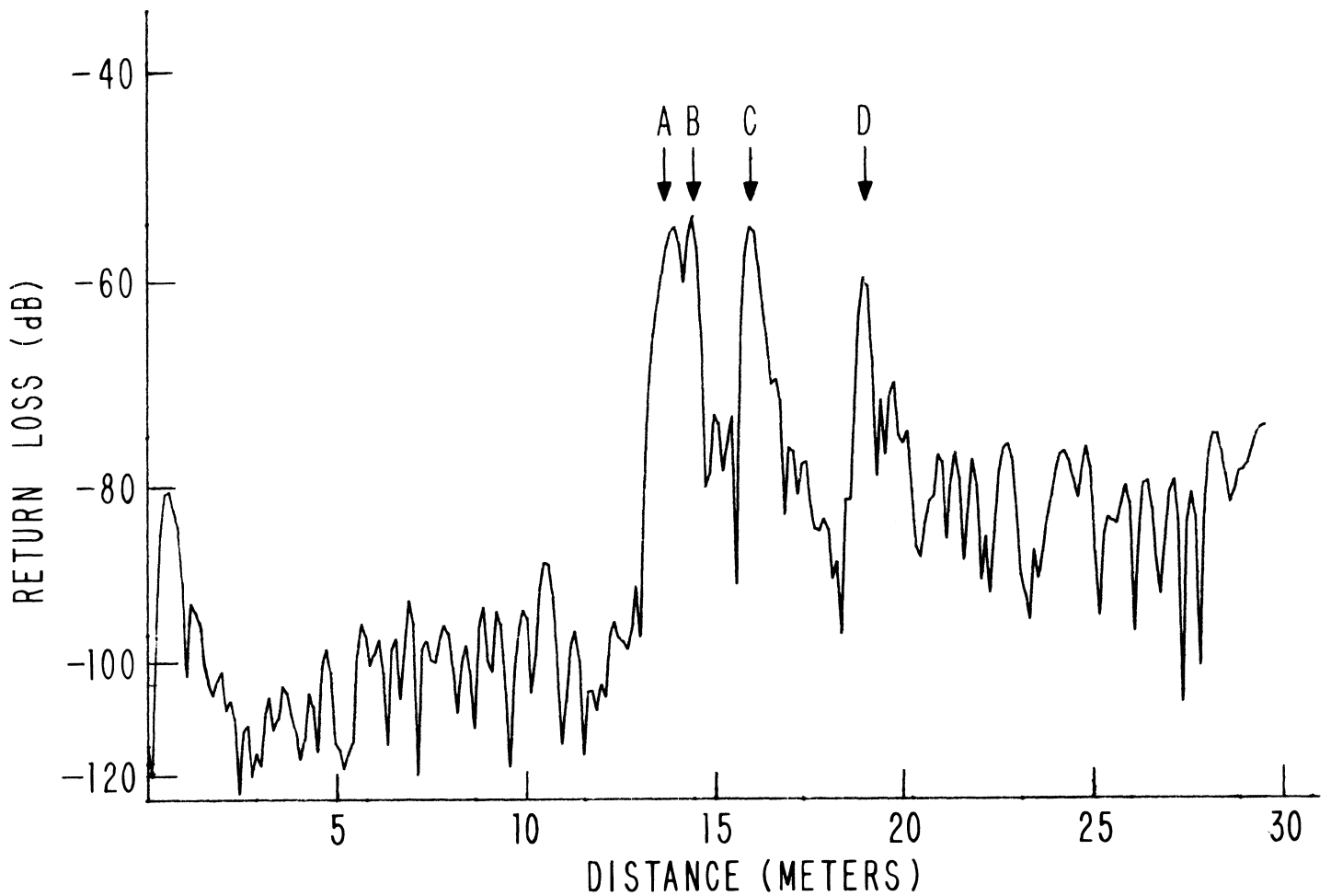


FIGURE 11. TOP OF THE 140-FOOT CASSEGRAIN HOUSE AS SEEN FROM THE FEED. THE SQUARE PLATE IS A TEMPORARY SPOILER COVERING THE L-BAND FEED WHICH IS ROUGHLY ON THE SOUTH SIDE OF THE HOUSE.



256 POINTS 3050 TO 3700 MHZ

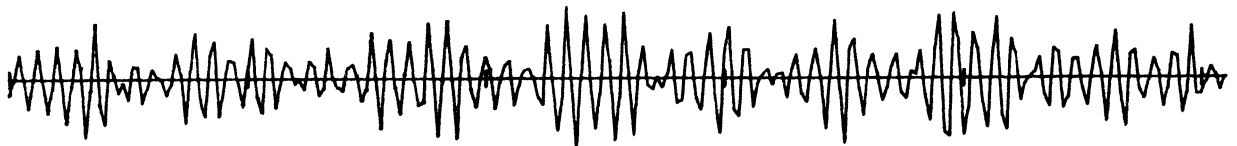
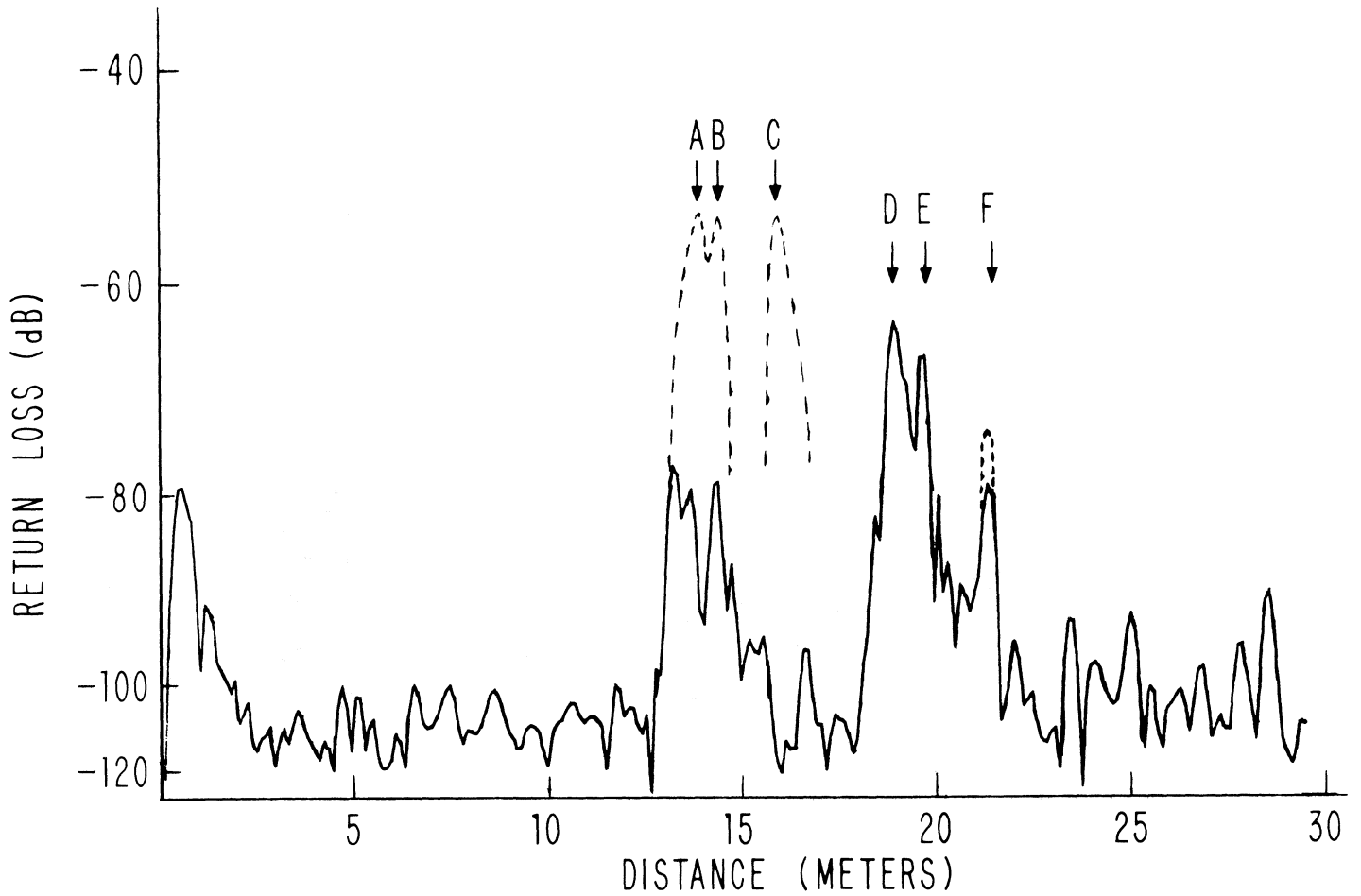


FIGURE 12. INTERFERENCE PATTERN BETWEEN INCOMING AND TRANSMITTED WAVES WITH VARYING FREQUENCY (BOTTOM) AND ITS FOURIER TRANSFORM (TOP) WHICH SHOWS THE RETURN LOSS (REFLECTION COEFFICIENT) AS A FUNCTION OF DISTANCE FROM THE REFLECTOMETER. THIS SPECTRUM WAS TAKEN ON THE 140-FOOT BEFORE ANY MODIFICATIONS WERE MADE TO SUPPRESS REFLECTIONS. REFLECTIONS ARE FROM (A AND B) THE TOP OF THE CASSEGRAIN HOUSE, (C) THE CASSEGRAIN FEEDS, AND (D) THE INNER DISH SURFACE.



256 POINTS 3050 TO 3700 MHZ

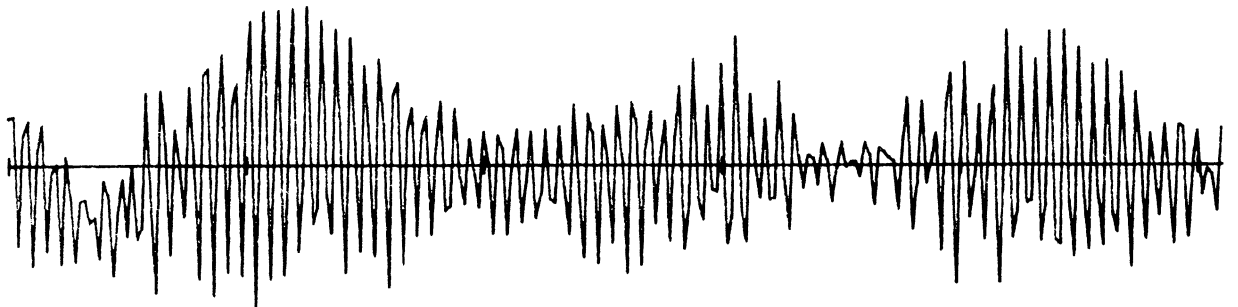


FIGURE 13. INTERFERENCE PATTERN AND RETURN LOSS-DISTANCE SPECTRUM FOR THE 140-FOOT WITH A SPOILER OVER THE L-BAND CASS FEED, ABSORBER OVER THE REST OF THE CASS HOUSE ROOF AND ALUMINUM TAPE OVER THE OUTER CRACK (F). DOTTED LINES SHOW REFLECTIONS BEFORE MODIFICATION, AND THE INTERFERENCE PATTERN SCALE IS EXPANDED TEN TIMES THAT IN FIGURE 12.

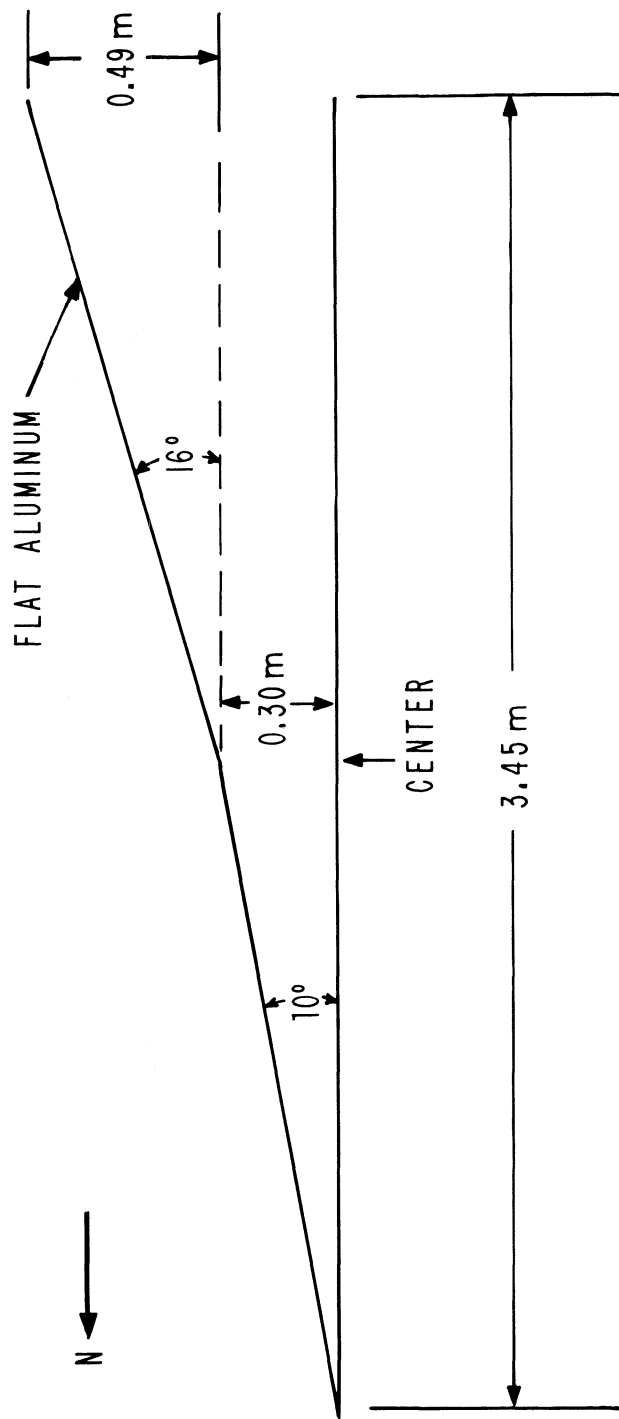
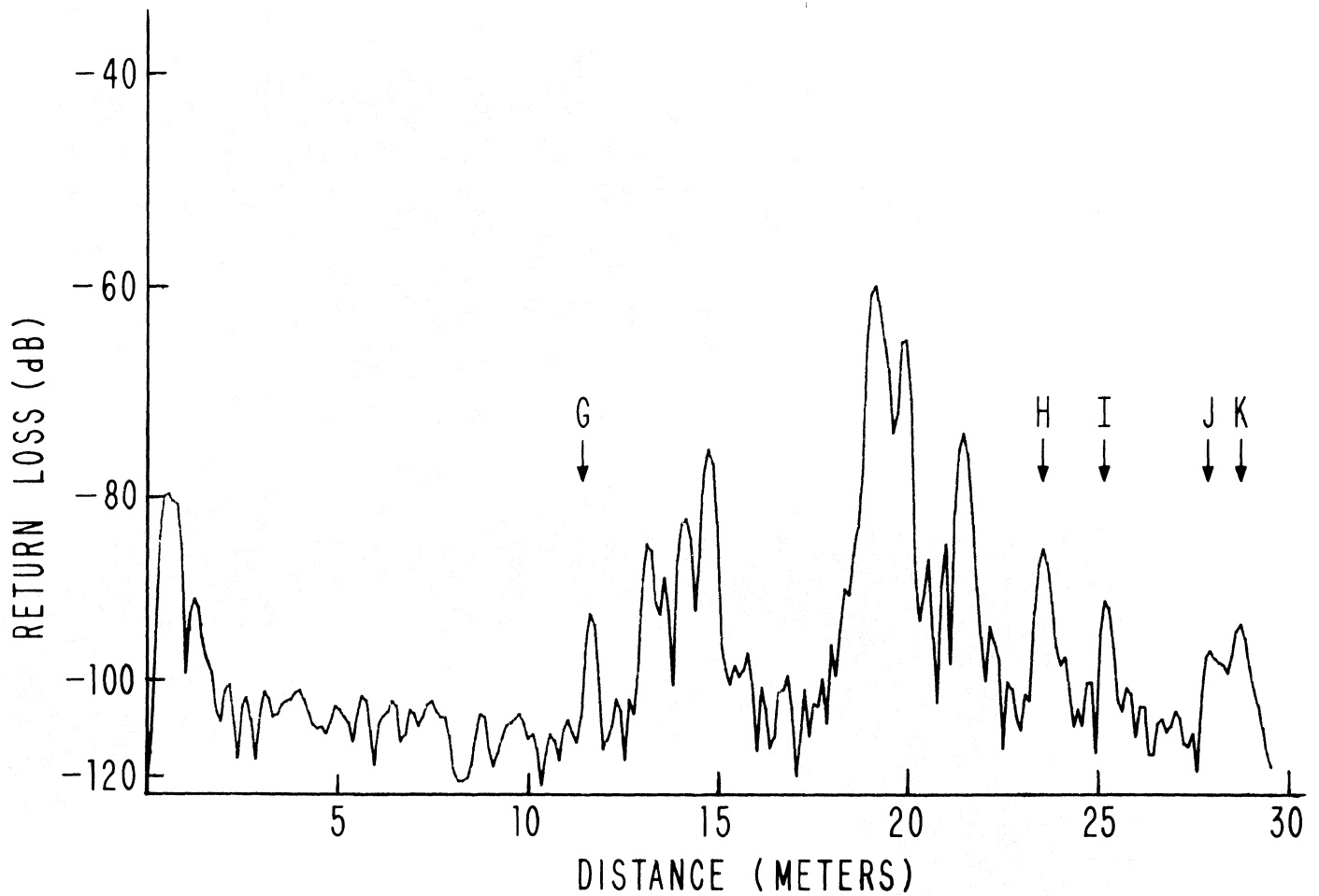


FIGURE 14. CROSS SECTION OF CIRCULAR SPOILER PLACED OVER THE TOP OF THE 140-FOOT CASSEGRAIN HOUSE. THE RESULTS ARE SHOWN IN FIGURE 15.



256 POINTS 3050 TO 3700 MHZ

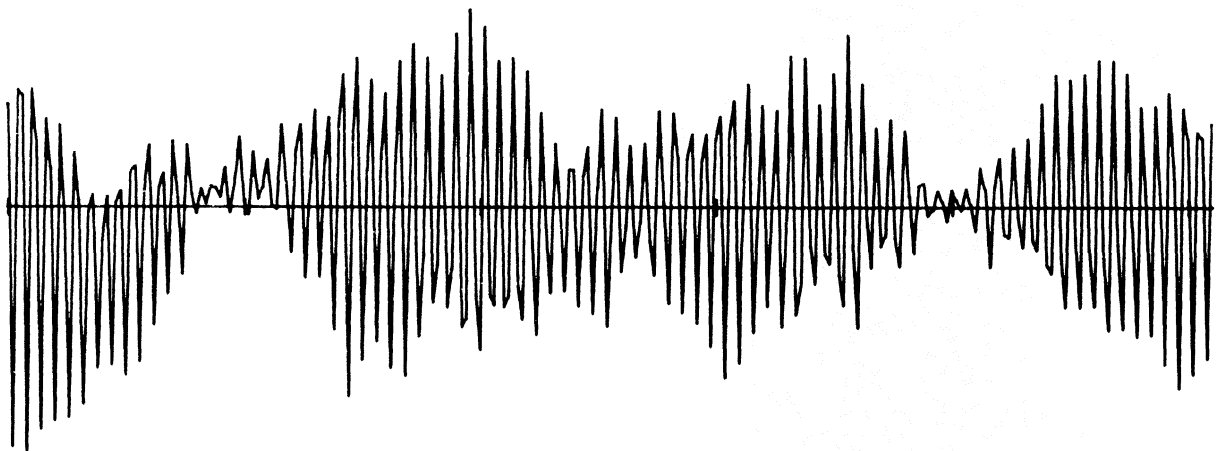


FIGURE 15. INTERFERENCE PATTERN AND REFLECTION SPECTRUM OF THE 140-FOOT WITH THE SPOILER OF FIGURE 14 IN PLACE. REFLECTION (G) IS FROM THE FEED LEG STIFFENING CABLES, AND (I) IS FROM THE EDGE OF THE DISH. THE SOURCES OF (H), (J), AND (K) HAVE NOT BEEN DETERMINED.

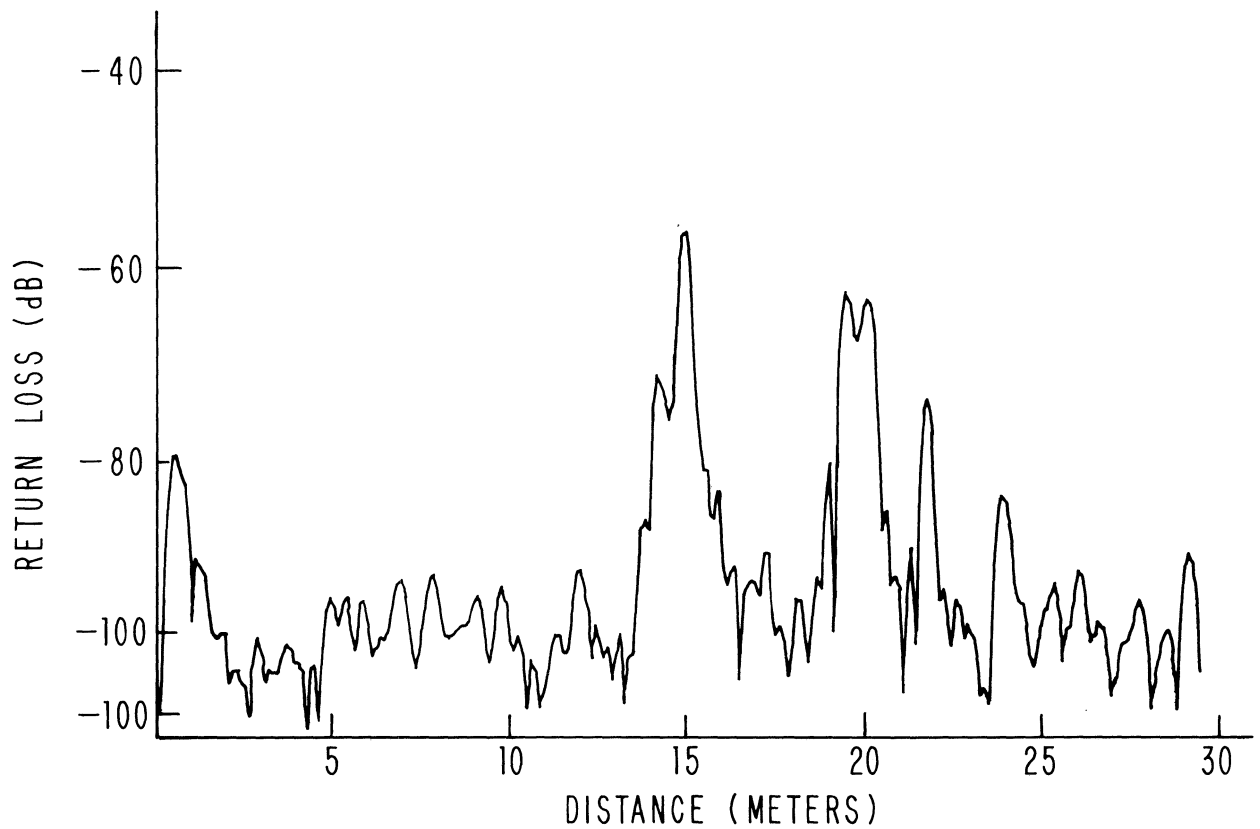
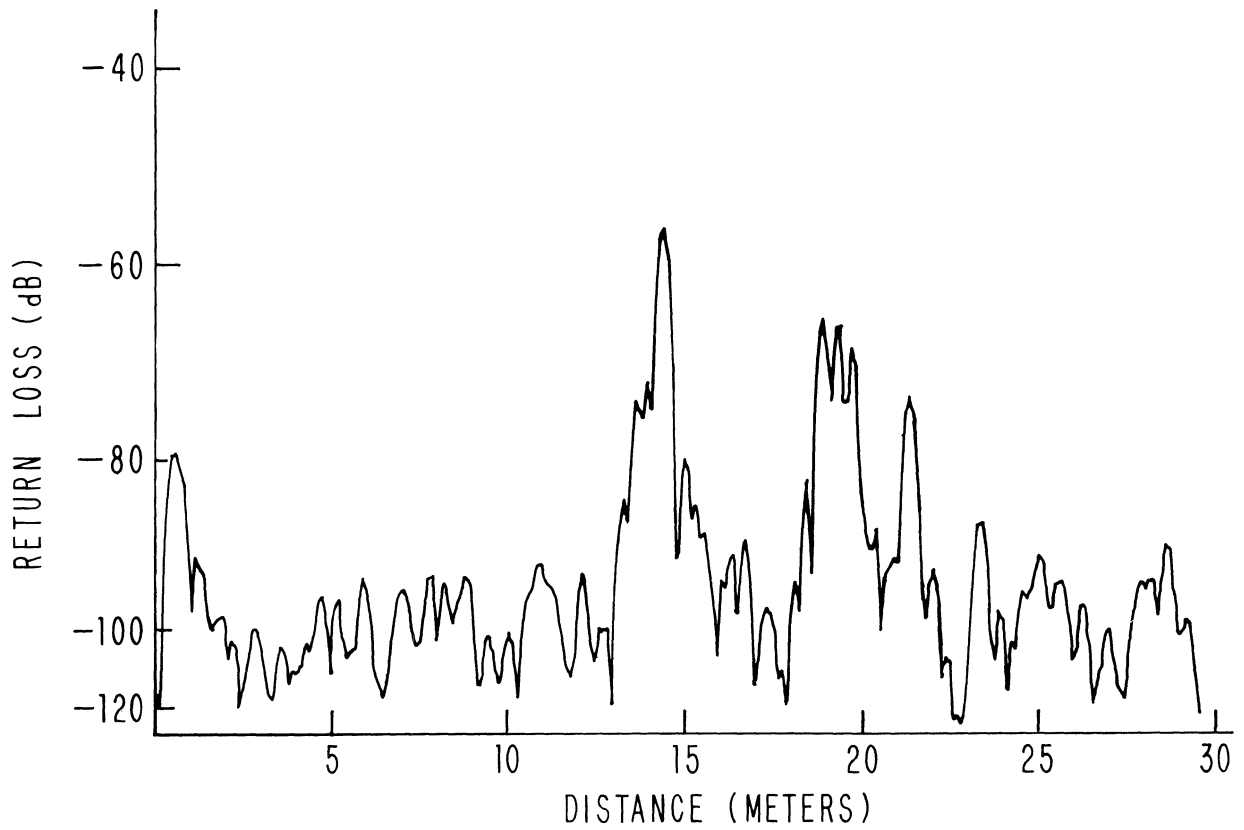


FIGURE 16. REFLECTION SPECTRA OF THE 140-FOOT SHOWING THE CHANGE IN REFLECTION CHARACTERISTICS AROUND 20 METERS (INNER DISH SURFACE) WITH A CHANGE IN AXIAL FEED POSITION. THE FEED FOR THE TOP PLOT WAS 55 CM FURTHER FROM THE DISH THAN IN THE BOTTOM PLOT.

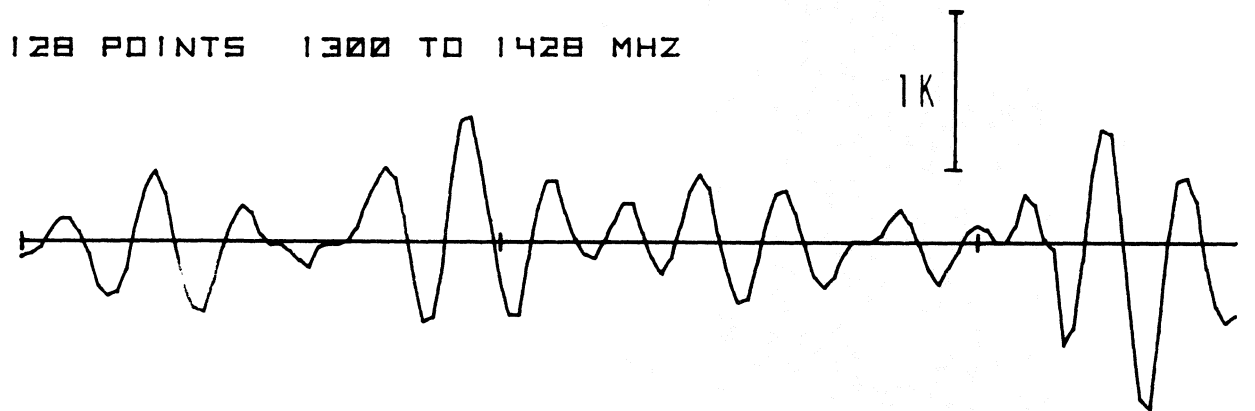
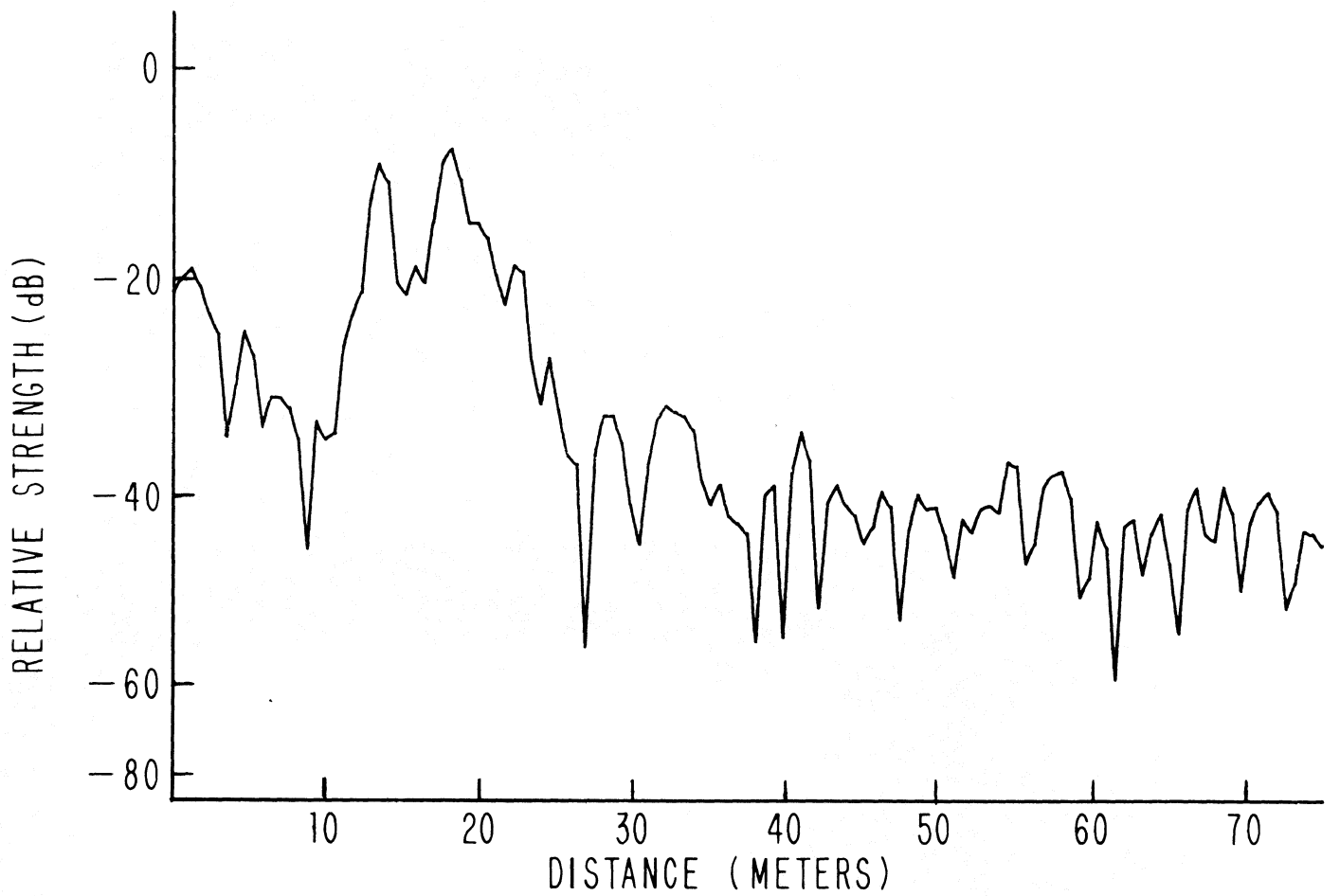


FIGURE 17. COMPOSITE 140-FOOT RADIOMETER BASELINE OVER 128 MHz (BOTTOM) AND ITS FOURIER TRANSFORM (TOP) FOR CHANNEL A OF THE 6/25 CM RADIOMETER WITH LINEAR POLARIZATION. THE BASELINE IS THE DIFFERENCE BETWEEN SPECTRA TAKEN $\lambda/8$ ABOVE AND BELOW THE NOMINAL FOCUS POSITION WITH THE ANTENNA POINTED AT THE ZENITH.

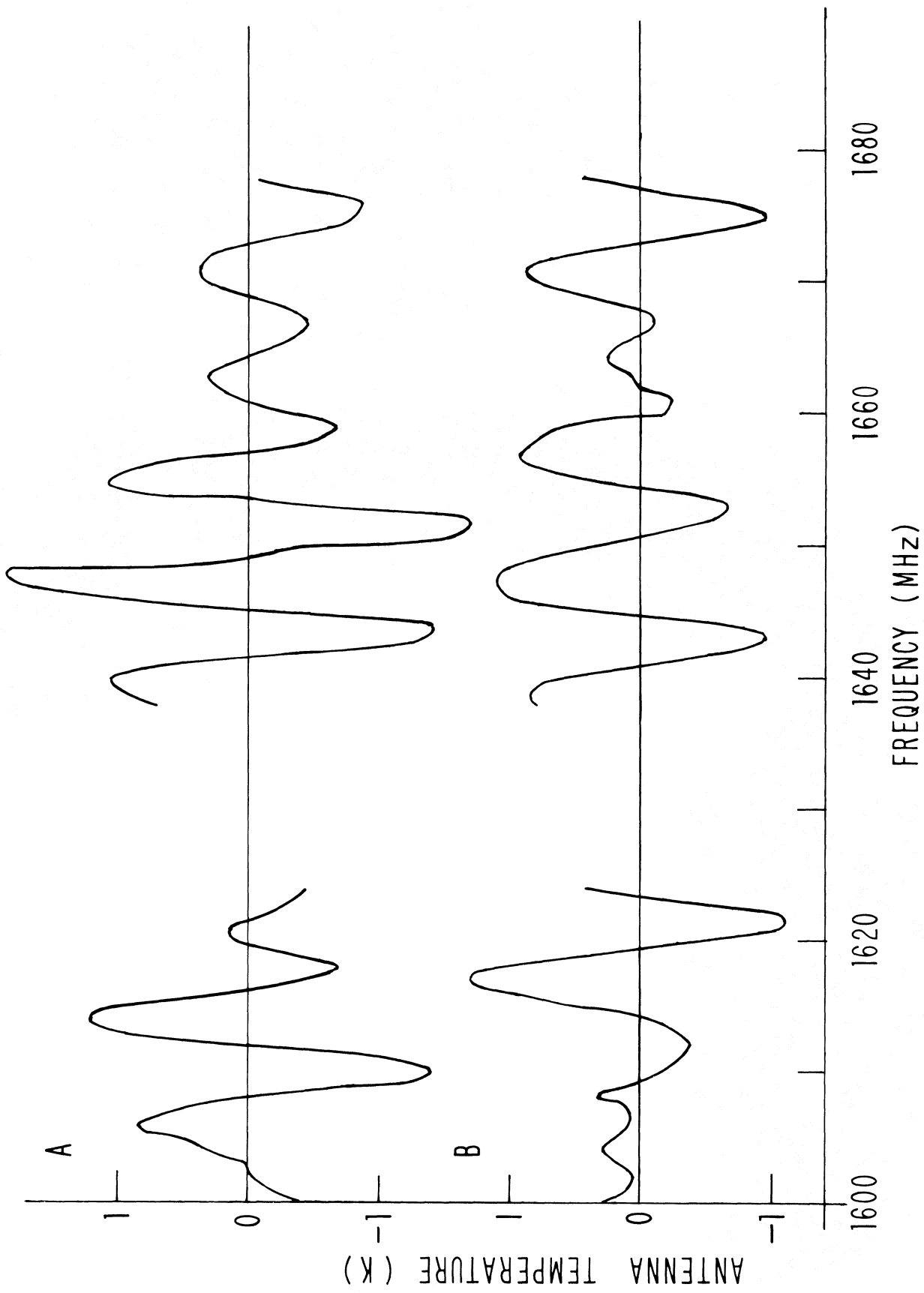


FIGURE 19. COMPOSITE 140-FOOT, 18 CM RADIOMETER BASELINES FOR BOTH ORTHOGONAL LINEARLY POLARIZED CHANNELS. THE BASELINES ARE THE DIFFERENCE BETWEEN SPECTRA TAKEN $\lambda/8$ ABOVE AND BELOW THE NOMINAL FOCUS POSITION WITH THE ANTENNA POINTED AT THE ZENITH.

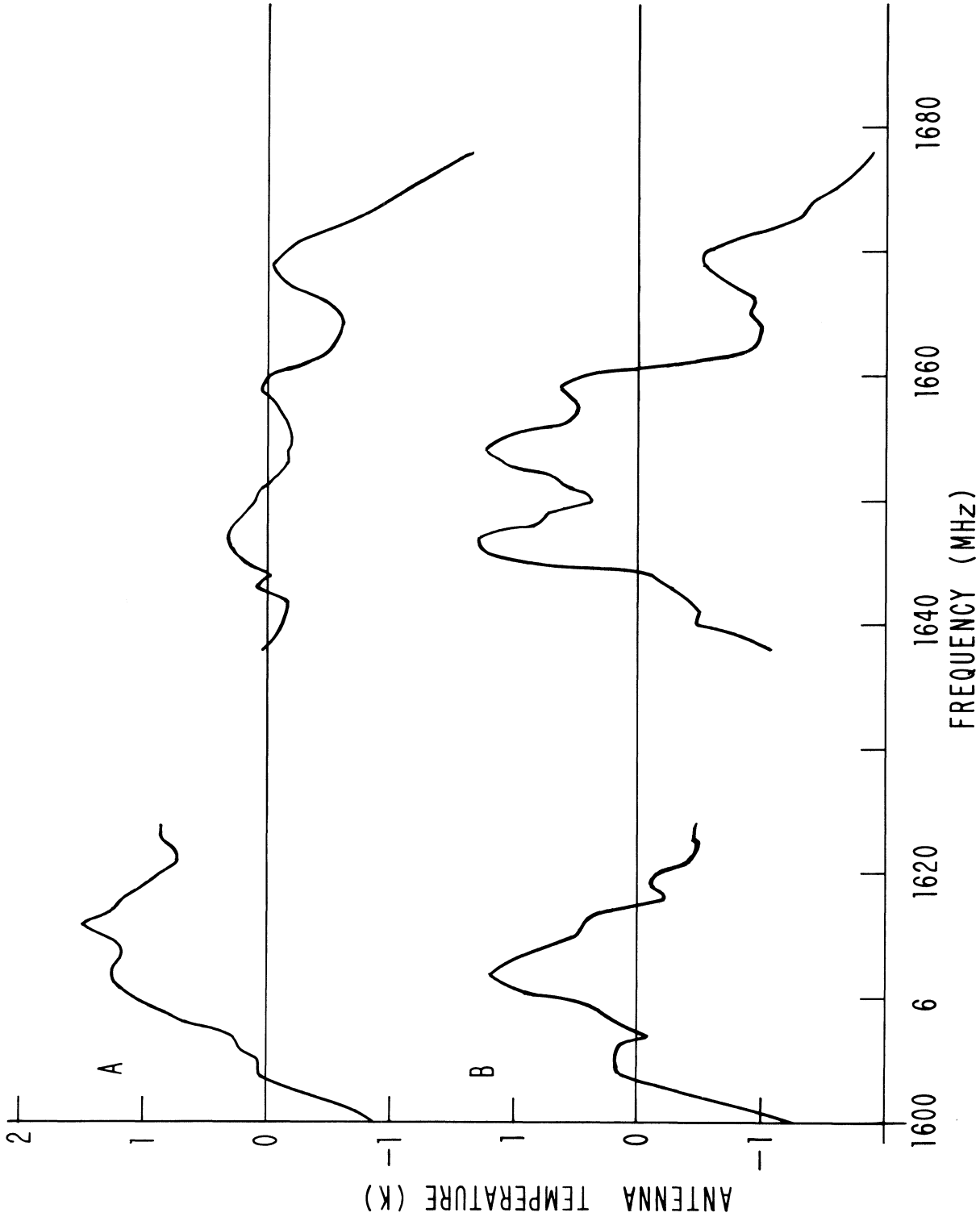
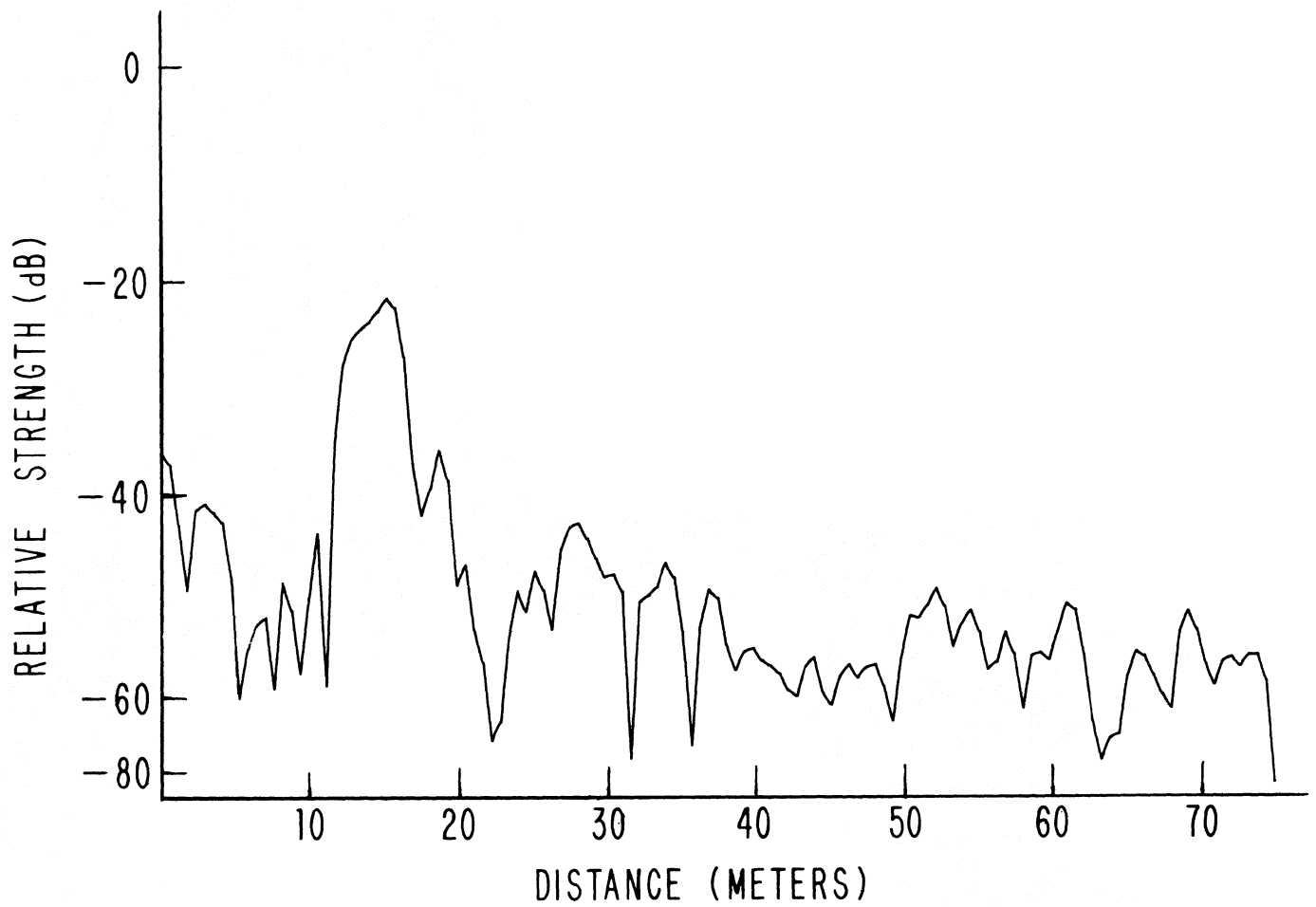


FIGURE 20. COMPOSITE 140-FOOT, 18 CM RADIOMETER BASELINES FOR BOTH ORTHOGONAL LINEARLY POLARIZED CHANNELS LOOKING AT 3C 274 WHICH PRODUCED AN ANTENNA TEMPERATURE OF ABOUT 50 K.



128 POINTS 3278 TO 3406 MHZ

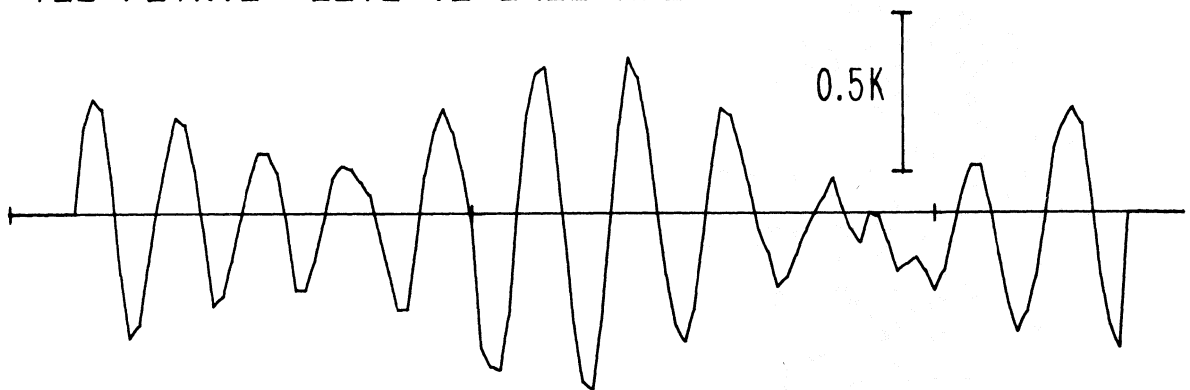


FIGURE 21. COMPOSITE 140-FOOT, 9 CM RADIOMETER BASELINE (BOTTOM) AND ITS FOURIER TRANSFORM. THE BASELINE IS THE DIFFERENCE BETWEEN SPECTRA TAKEN $\lambda/8$ ABOVE AND BELOW THE NOMINAL FOCUS POSITION WITH THE ANTENNA POINTED AT THE ZENITH.

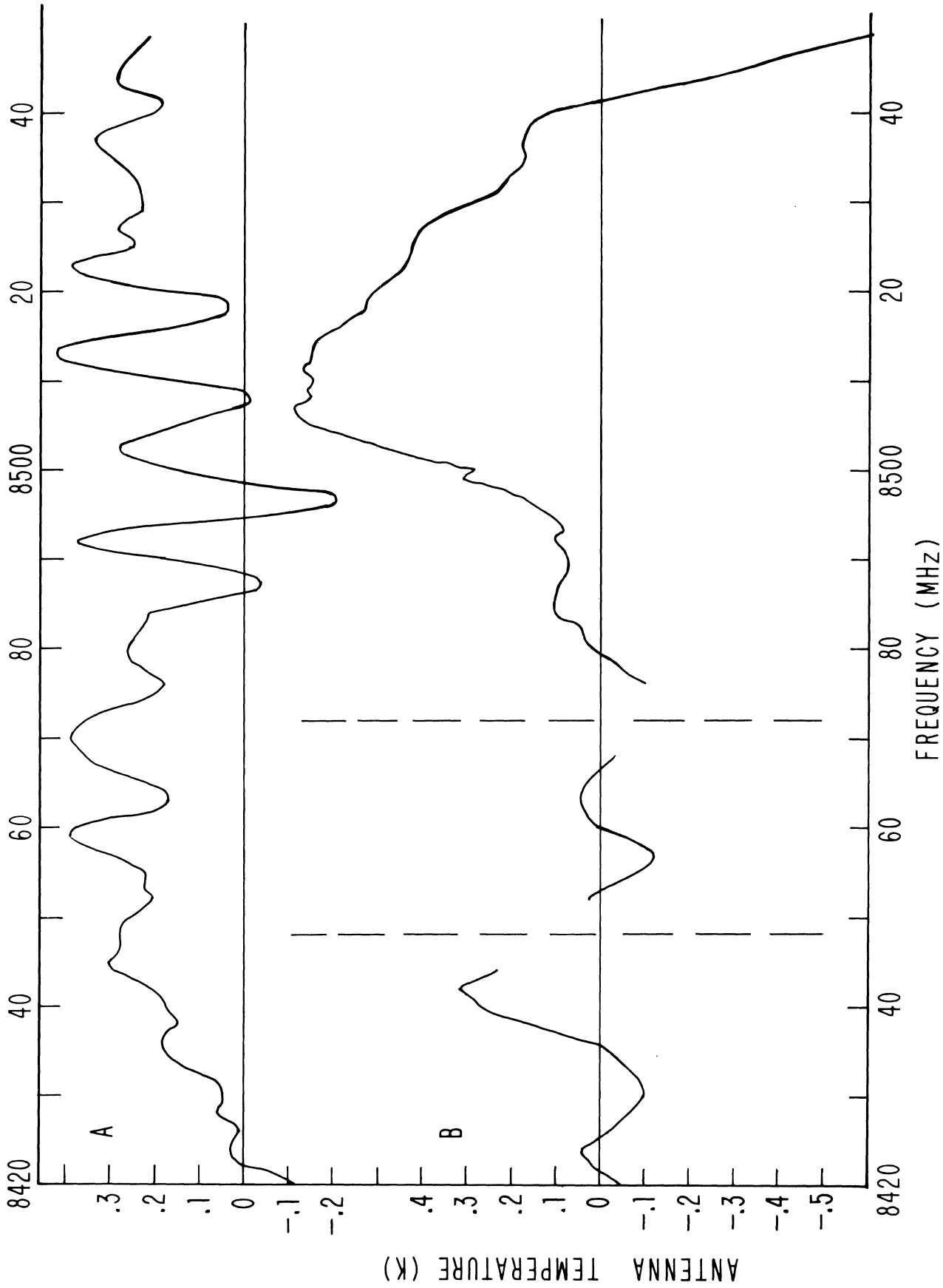


FIGURE 22. COMPOSITE 140-FOOT, 3.5 CM RADIOMETER BASELINES. THE BASELINES ARE THE DIFFERENCE BETWEEN SPECTRA TAKEN (A) $\lambda/8$ ABOVE AND BELOW THE NOMINAL FOCUS POSITION WITH THE ANTENNA POINTED AT THE ZENITH AND (B) ON AND OFF OF THE SOURCE 3C 147.1.

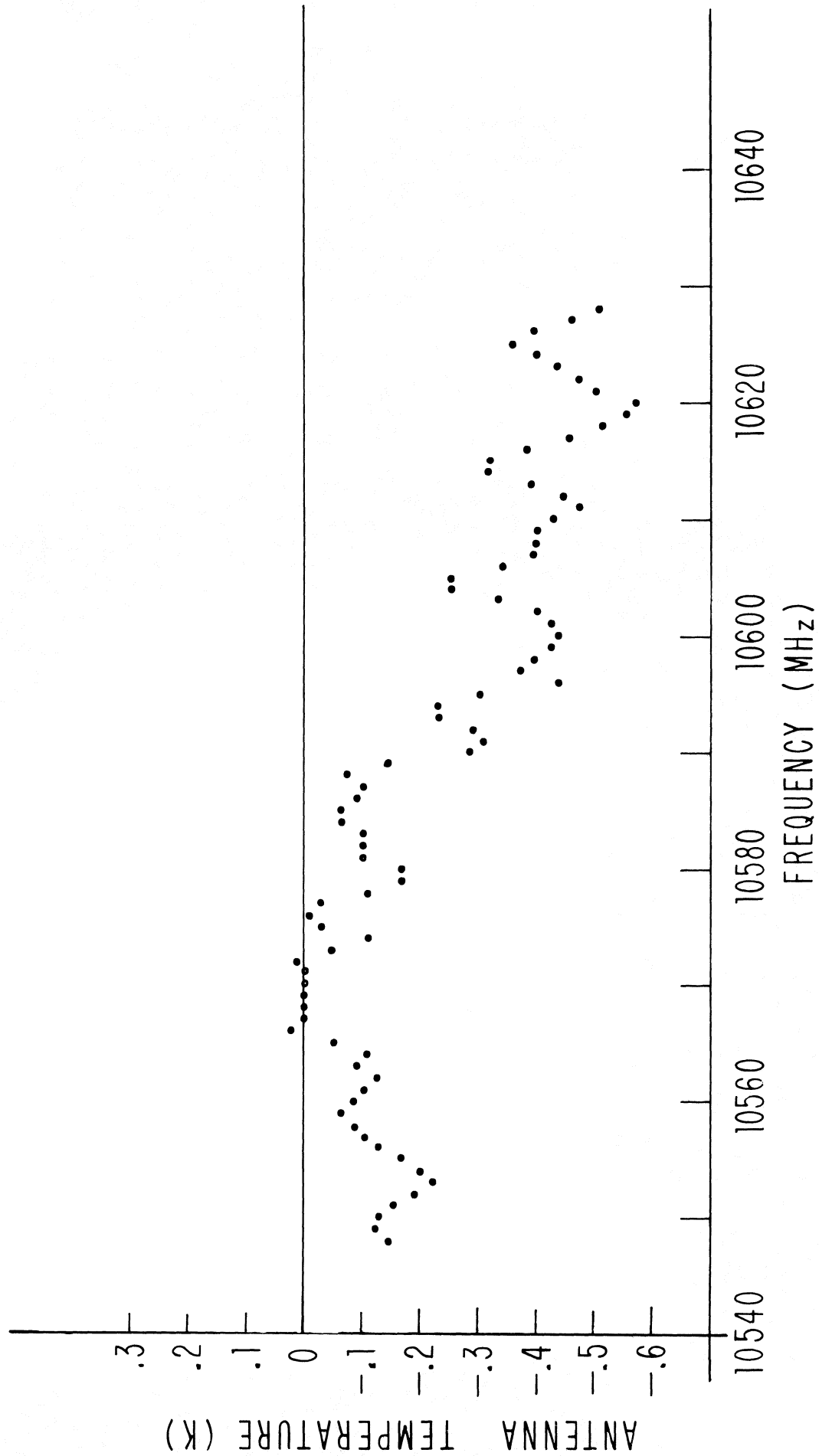


FIGURE 23. COMPOSITE 140-FOOT, 2.8 CM RADIOMETER BASELINE. THE BASELINE IS THE DIFFERENCE BETWEEN SPECTRA TAKEN $\lambda/8$ ABOVE AND BELOW THE NOMINAL FOCUS POSITION WITH THE ANTENNA POINTED AT THE ZENITH.

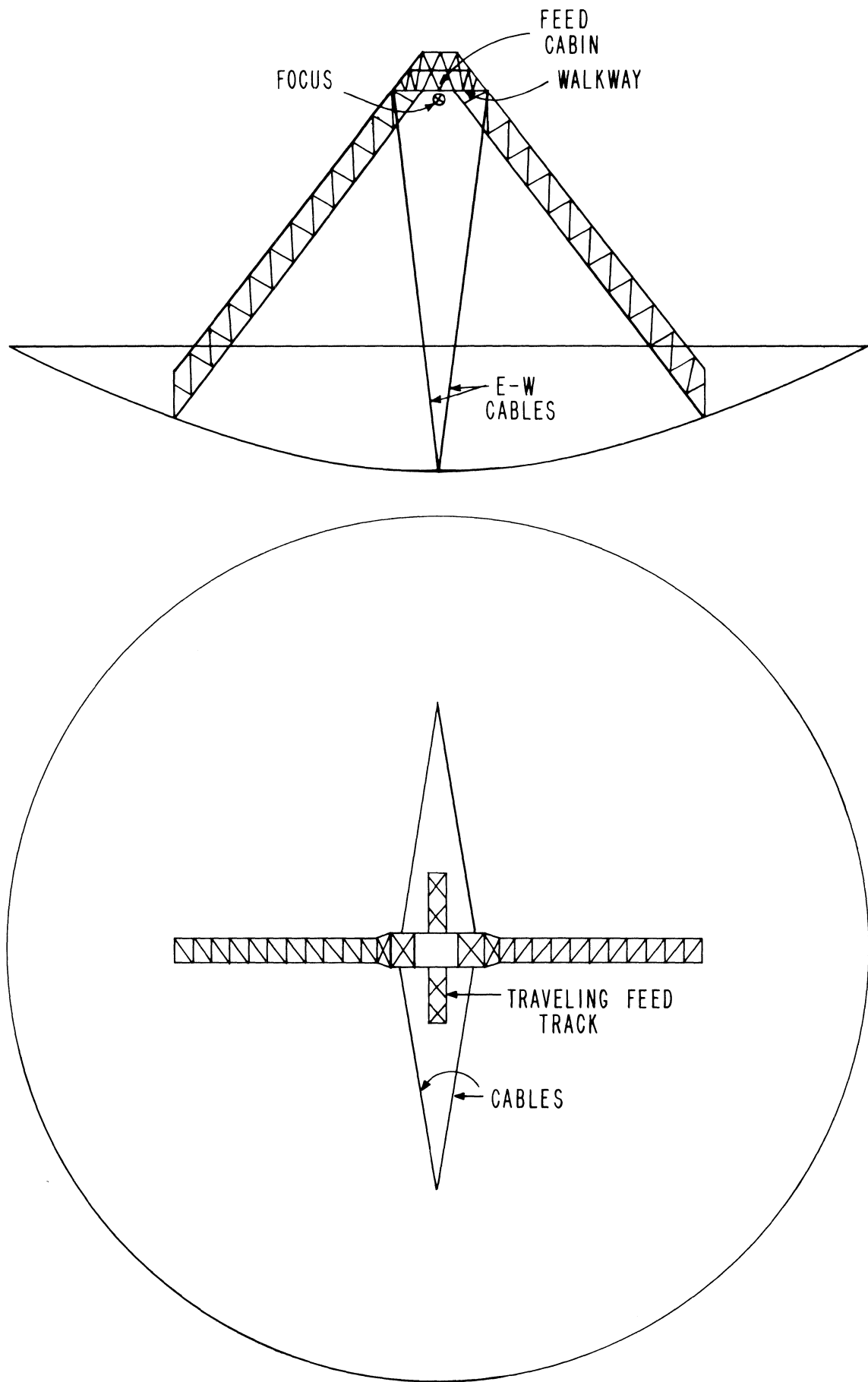


FIGURE 24. SCHEMATIC CROSS SECTION AND PLAN VIEW OF THE 300-FOOT TELESCOPE.

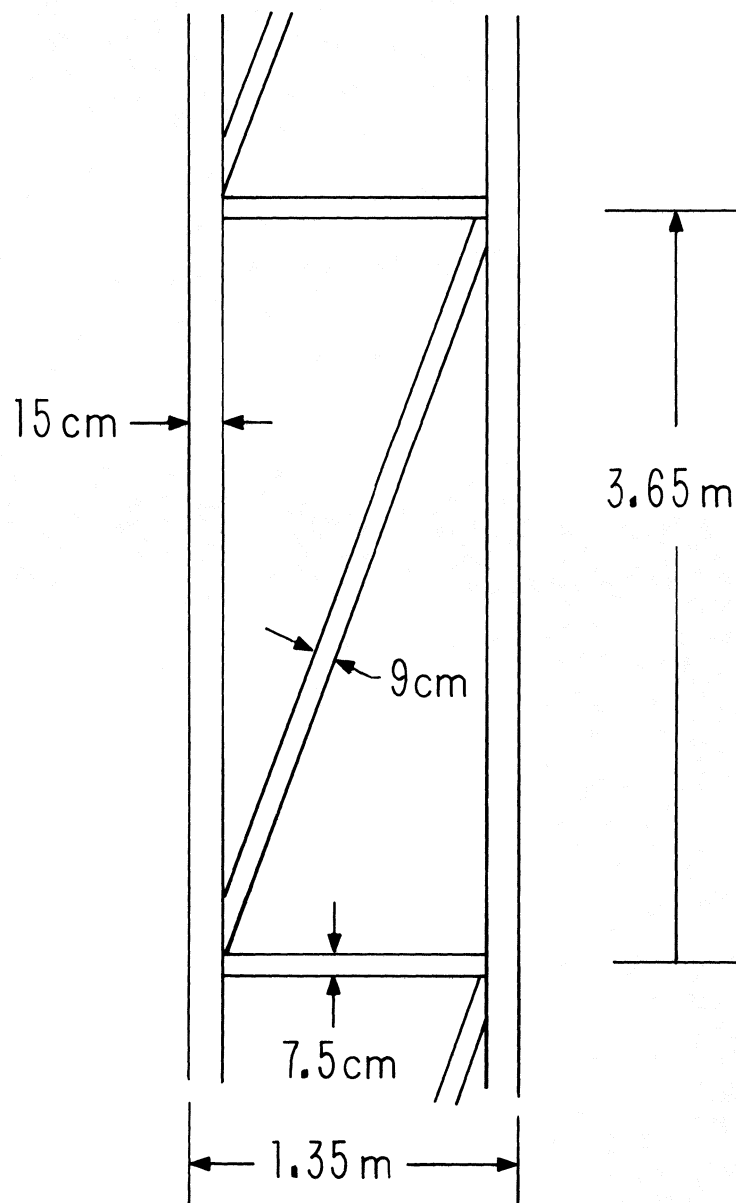


FIGURE 25. DETAILS OF THE INSIDE SURFACE OF THE 300-FOOT FEED SUPPORT LEGS. ALL MEMBERS ARE SQUARE TUBING WITH ONE SURFACE IN THE PLANE OF THE DRAWING. THE OUTSIDE SURFACE OF THE LEGS HAS ROUGHLY THE SAME CONSTRUCTION EXCEPT THAT THE TOTAL WIDTH IS ABOUT 2.3 METERS. THE LEGS FLARE SOMEWHAT NEAR THE TOP TO MATE WITH THE FEED CABIN.

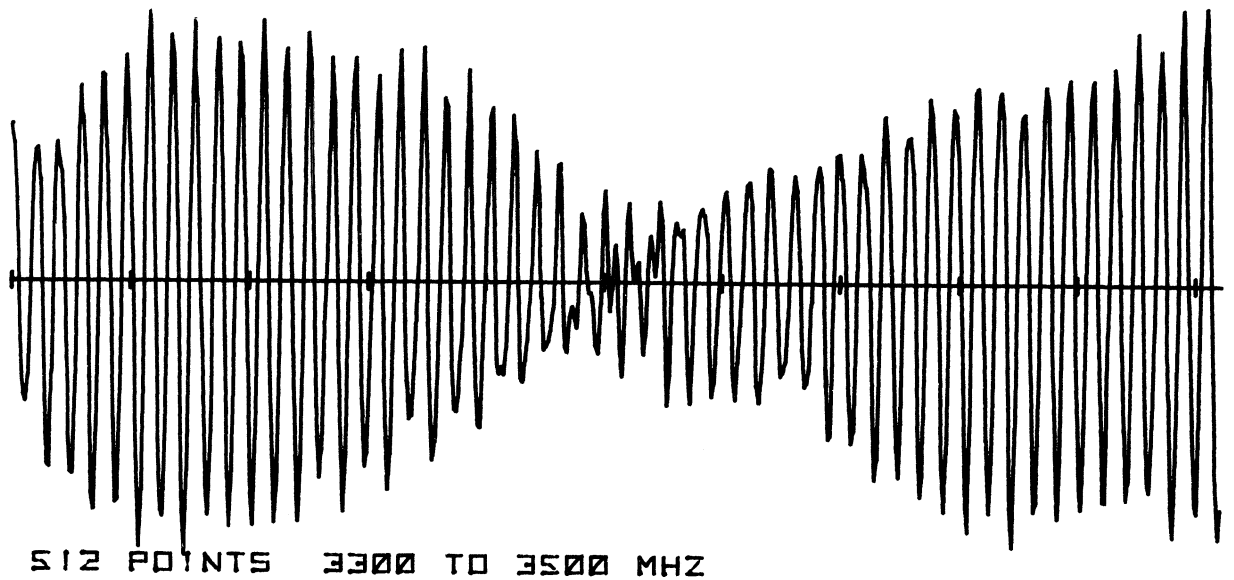
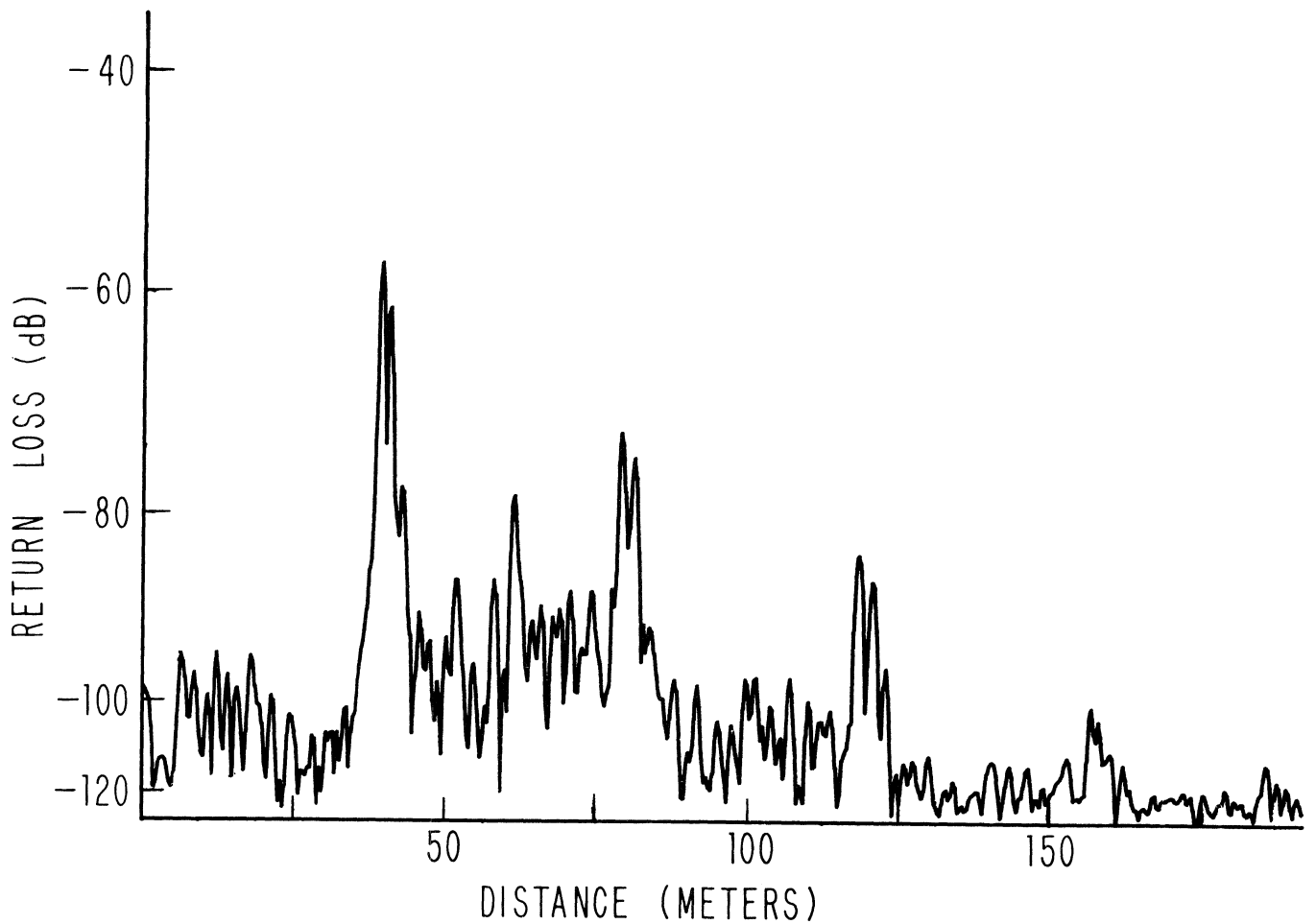


FIGURE 26. INTERFERENCE PATTERN AND REFLECTION SPECTRUM OF THE 300-FOOT TELESCOPE BEFORE ANY MODIFICATIONS. THE REFLECTION AT ABOUT 39 METERS IS FROM THE CENTRAL DISH SURFACE, AND THE HARMONICS ARE MULTIPLE BOUNCES BETWEEN THE SURFACE AND STRUCTURE NEAR THE FEED CABIN.

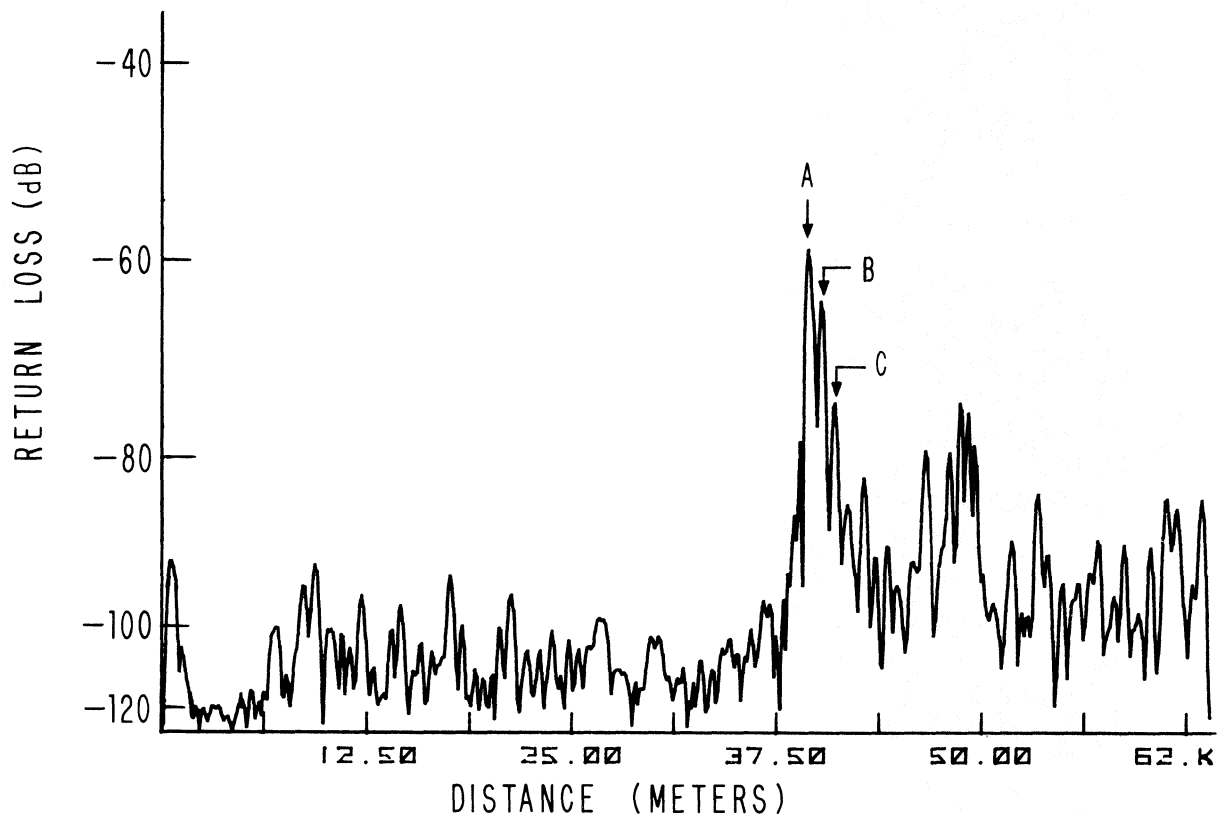
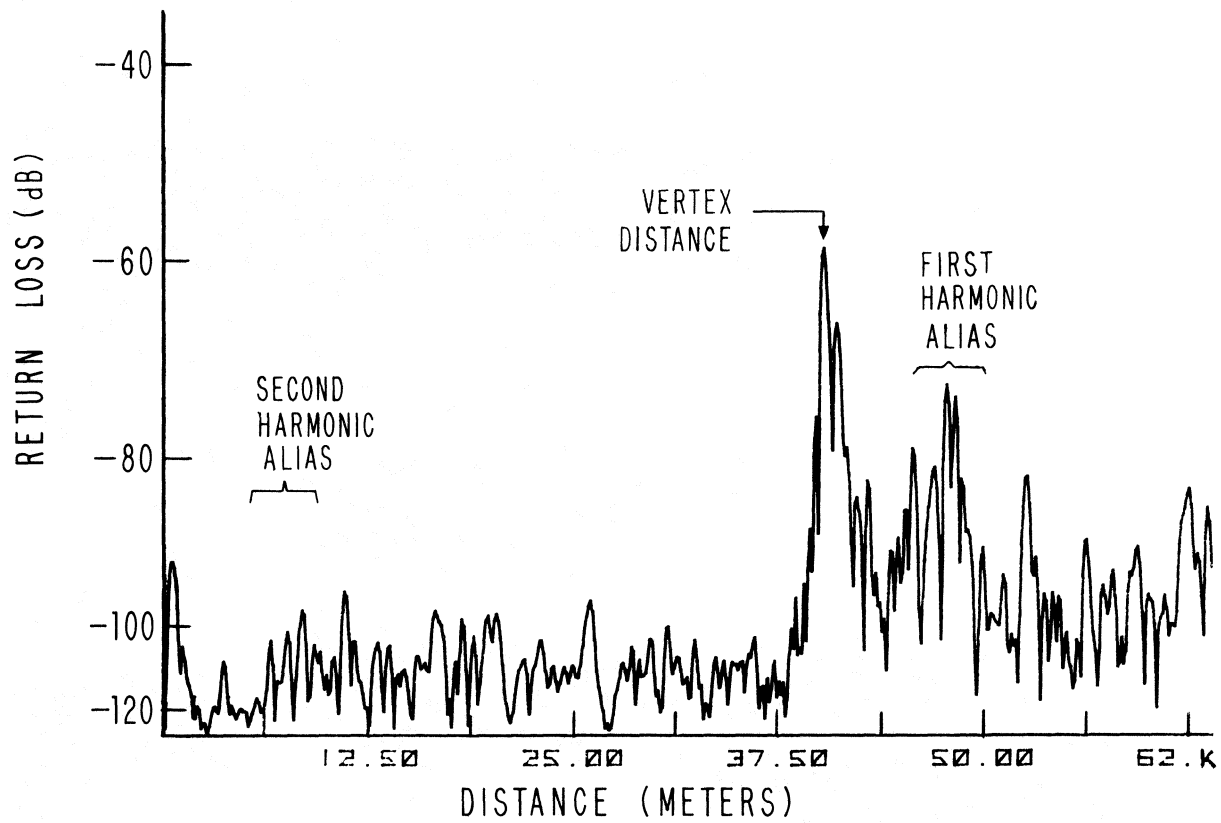
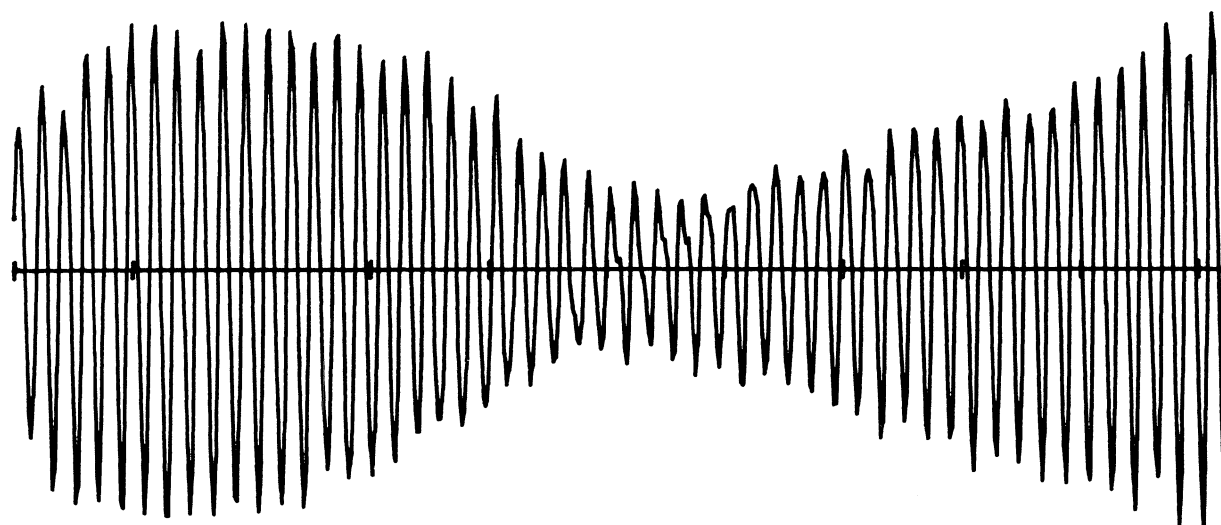
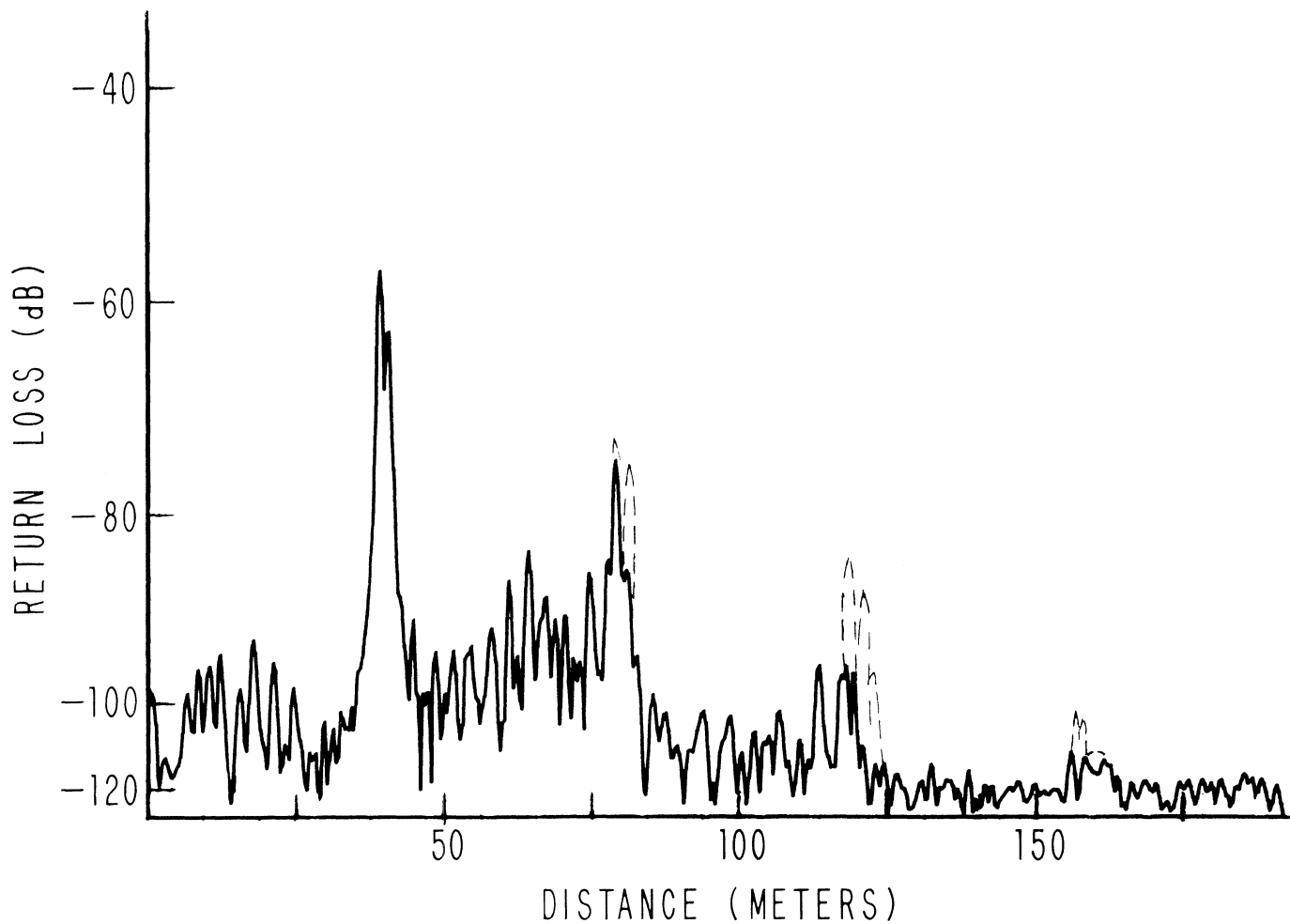


FIGURE 27. EXPANDED VIEW OF THE 300-FOOT REFLECTION SPECTRUM IN FIGURE 26 WITH THE FEED IN TWO DIFFERENT POSITIONS ALONG THE AXIS OF THE TELESCOPE. THE FEED WAS 87 CM FURTHER FROM THE DISH IN THE TOP PLOT THAN IN THE BOTTOM ONE.



512 POINTS 3300 TO 3500 MHZ

FIGURE 28. REFLECTION SPECTRUM OF THE 300-FOOT WITH ABSORBER COVERING THE BOTTOM OF THE FEED CABIN. THE DASHED LINES SHOW THE REFLECTIONS WITHOUT ABSORBER.

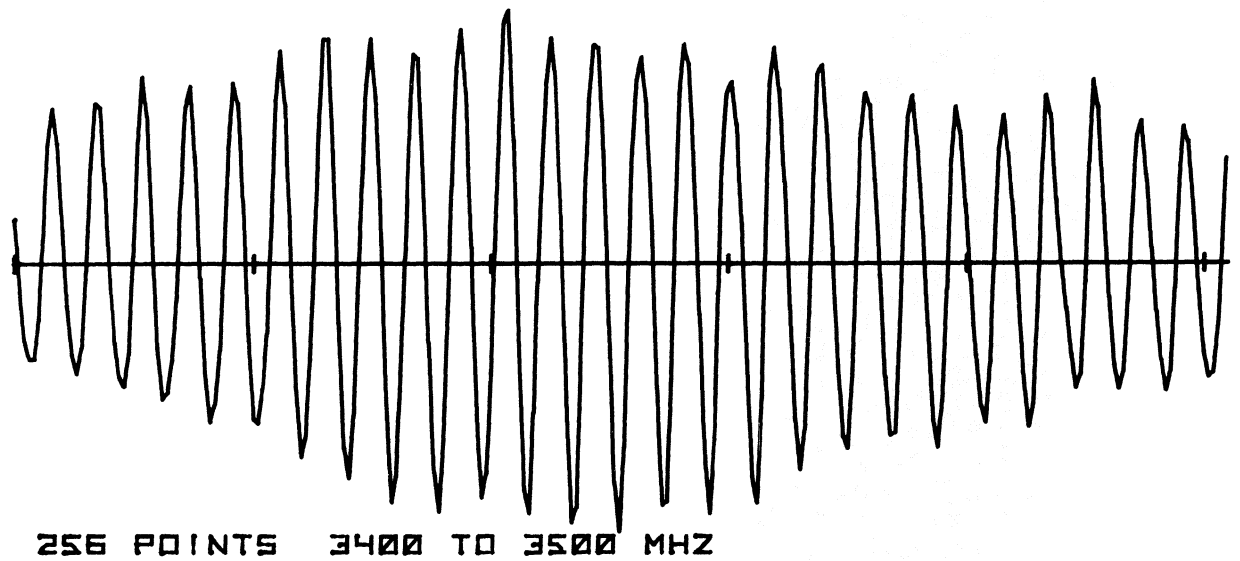
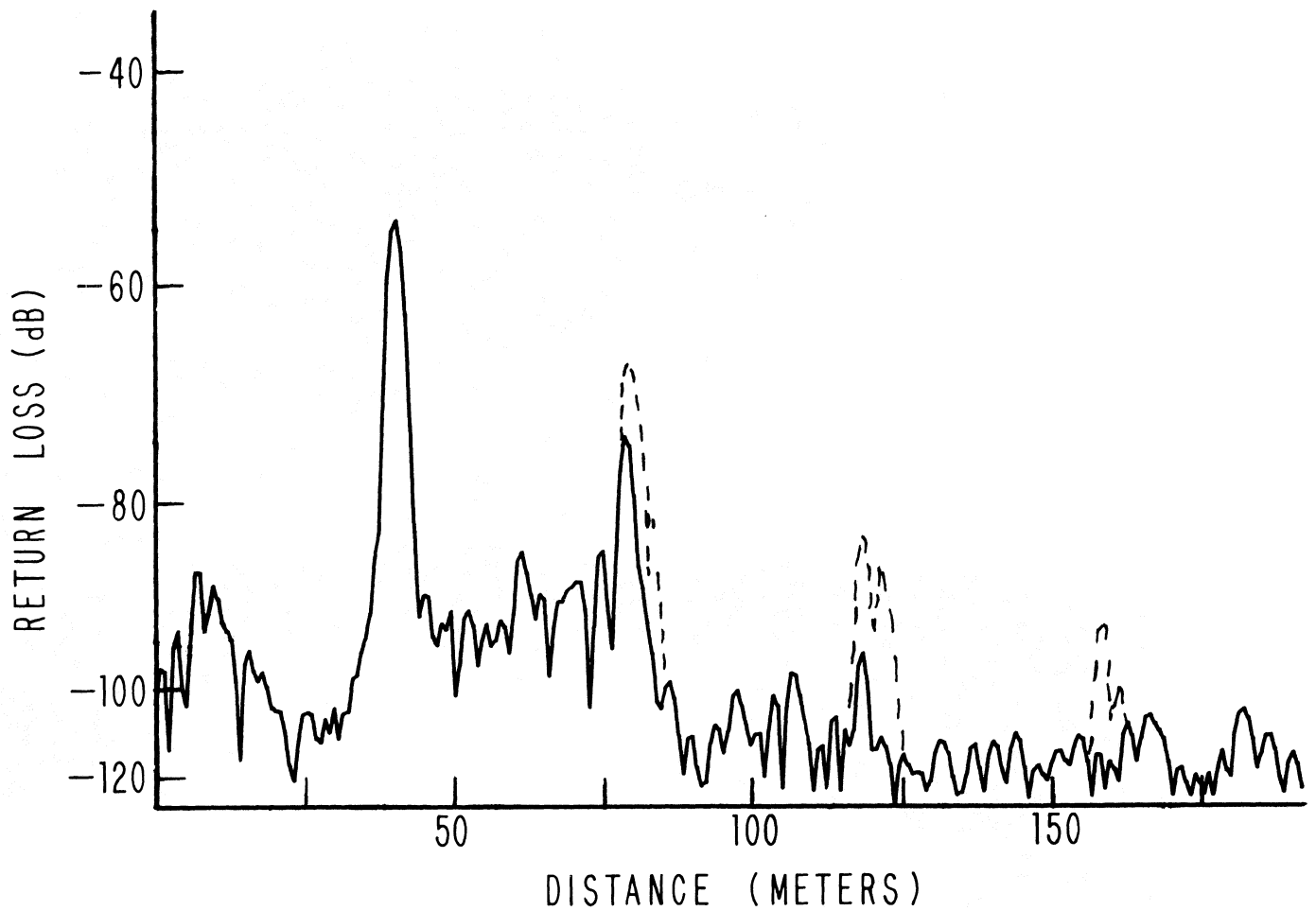


FIGURE 29. REFLECTION SPECTRUM OF THE 300-FOOT WITH A TILTED FLAT SPOILER AT THE CENTER OF THE DISH. THE DASHED LINES SHOW THE REFLECTIONS WITHOUT THE SPOILER. THE RESOLUTION IS HALF THAT OF THE OTHER 300-FOOT SPECTRA.

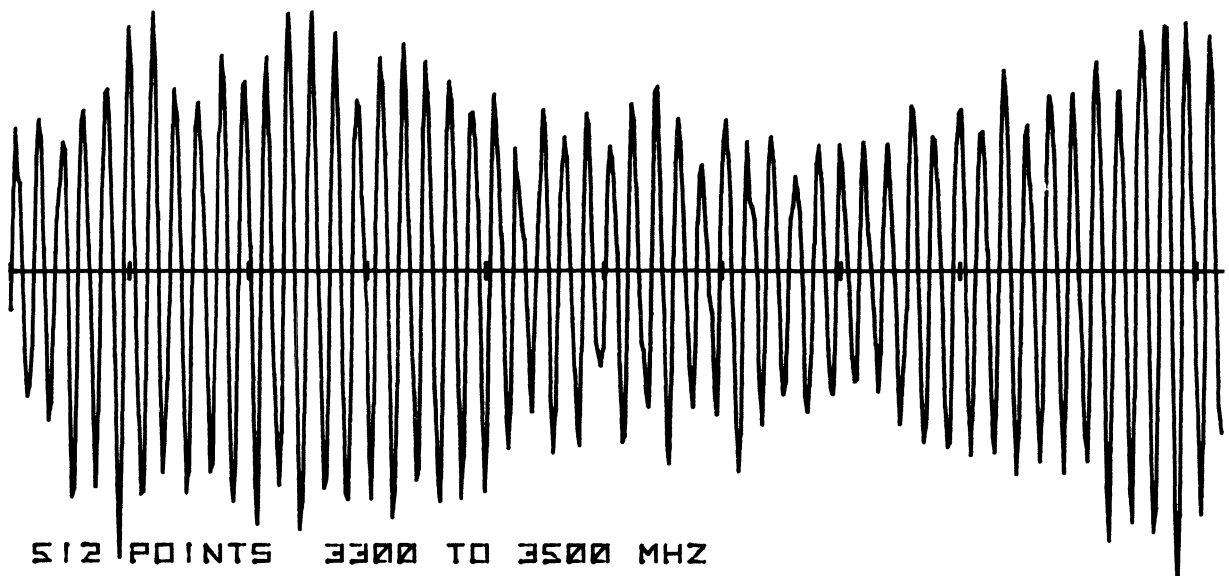
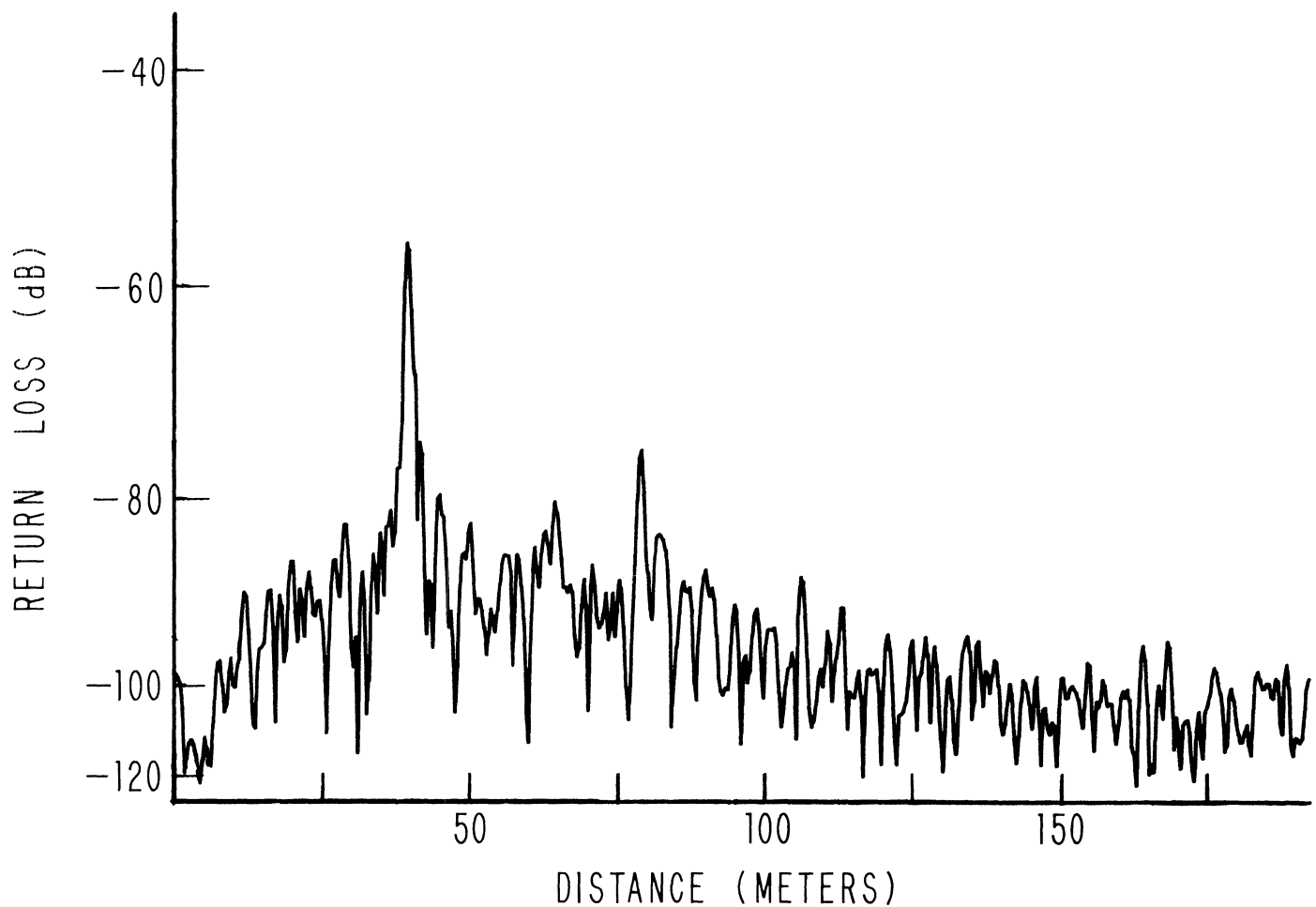
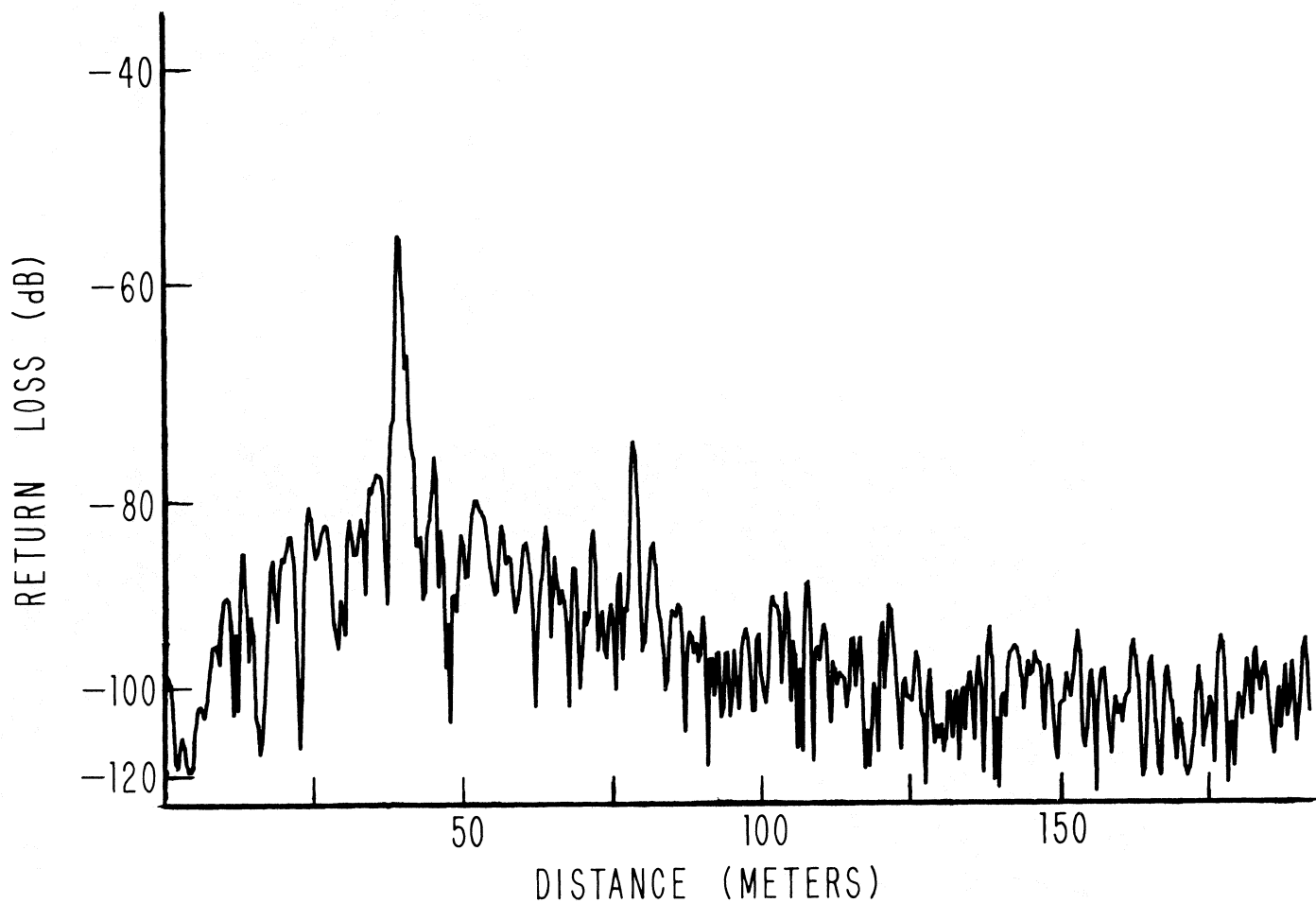


FIGURE 30. REFLECTION SPECTRUM OF THE 300-FOOT WITH ABSORBER UNDER THE FEED CABIN AND WIRE SCREENS ON THE INSIDE OF THE TOP OF THE FEED SUPPORT LEGS TO SHIELD THE WALKWAYS FROM THE SURFACE. THE HIGHER NOISE LEVEL IS DUE TO THE MOVEMENT OF THE SCREENS IN THE WIND.



512 POINTS 3300 TO 3500 MHZ

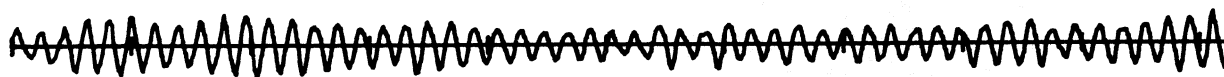


FIGURE 31. REFLECTION SPECTRUM OF THE 300-FOOT WITH ABSORBER UNDER THE FEED CABIN, WIRE SCREEN SPOILERS UNDER THE WALKWAYS, AND TILTED SCREENS ON THE SURFACE UNDER THE TRAVELING FEED TRACKS.

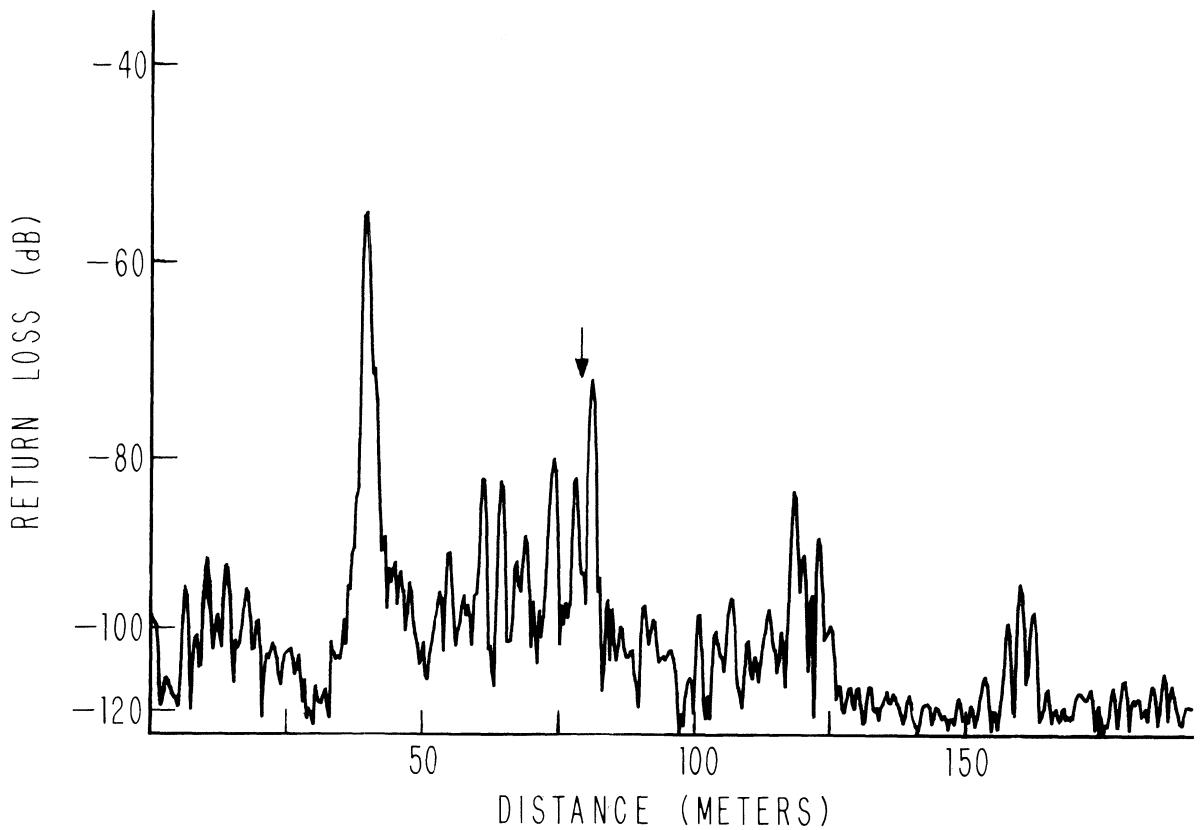
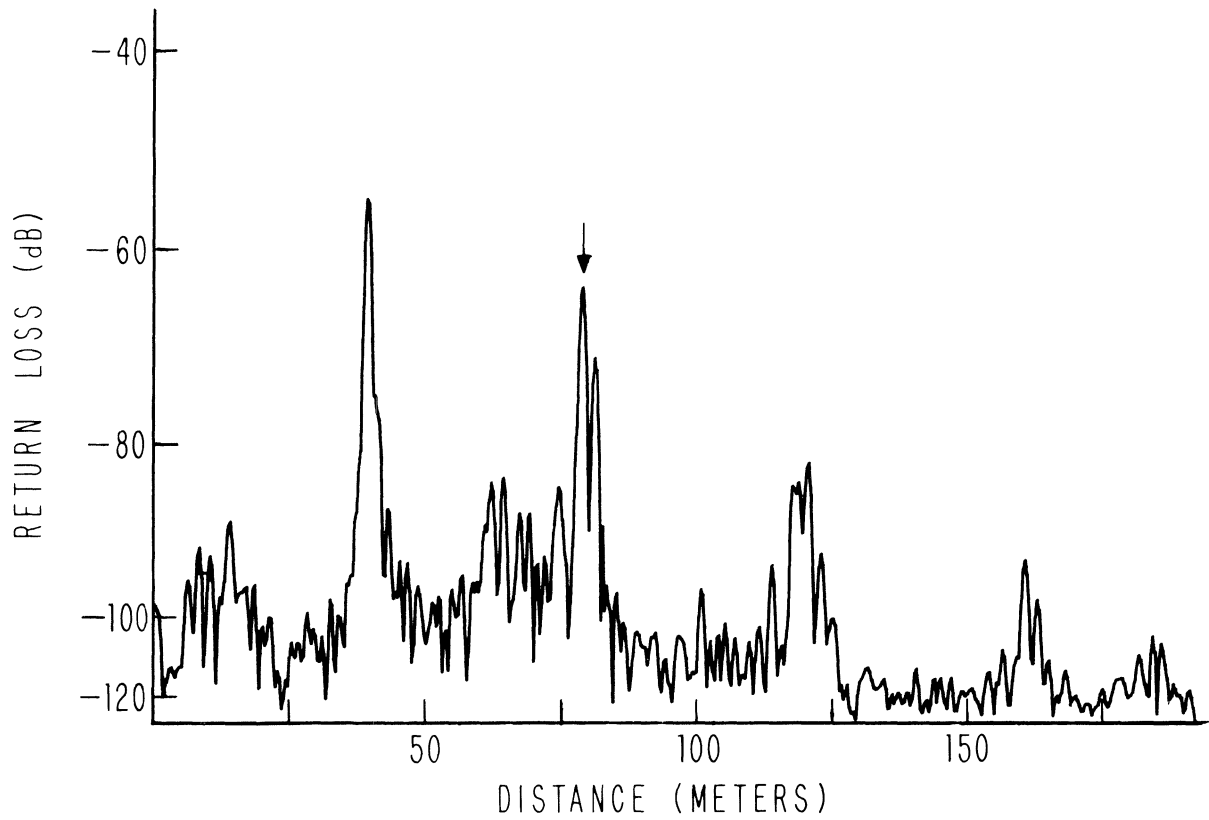


FIGURE 32. REFLECTION SPECTRA OF THE 300-FOOT WITH THE FEED 38 CM WEST (TOP) AND EAST (BOTTOM) OF THE TELESCOPE AXIS. THE ARROWS MARK A DOUBLE BOUNCE FEATURE WHICH IS VERY DEPENDENT ON LATERAL FEED POSITION.